University of Bremen

AG MSIS

Multi-Sensor Interactive Systems Group

State Estimation Solely Based on Prior Knowledge and Inertial Sensors

PhD Thesis

Computer Science

Tom L. Koller

First Examiner & Supervisor: Prof. Dr.-Ing. Udo Frese
(University of Bremen)

Second Examiner: Prof. Dr.-Ing. Thomas Seel
(Friedrich-Alexander-University of Erlangen-Nürnberg)

Defended at 14.11.2022

Where am I?

Where am I? I am at a milestone in the long journey to learn the ins and outs of science. I am writing and refining the last parts of this thesis to attain a PhD. Somehow it feels like the end of a path, although it is just a certificate — a certificate that proofs the ability to perform self-reliant science. While the ”self” is quite important, I would not stand here without the guidance and support of the people I met at my journey.

I am grateful for all those who guided, taught, supervised, examined, entertained, comforted, invited, amazed, motivated, enlightened, advised, distracted, scolded, debunked, exhausted, attended, supported, dined with, joked with, laughed with, discussed with, watched with, pondered with, celebrated with, stayed with, danced with, exercised with, chanted with, played with, worked with, studied with, traveled with, dreamed up with, consulted with, cringed with, loafed with, cheered with, cooked for, or listened to me. You helped me to overcome the inevitable obstacles of this thesis.

Furthermore, I am much obliged to the reviewers of my thesis who found many typos, grammar mistakes and brain twisters. They greatly aided me to improve the comprehensibility of this work. Last but not least, I want to honor the efforts of my co-authors in this cumulative thesis, wherefore I use the ”We” when I review our results.

You may ask for whom this work is, but that is a simple matter. It is a work of and for science!

Abstract

How do we localize ourselves? Ever since GPS exists, it is common to know where we are and how to get to our desired location. Unfortunately, GPS is unavailable indoors. Scientists are looking for an alternative technology that can fill this localization gap. One approach is to fuse knowledge about our environment and our movement measured with inertial sensors. A particular difficulty of these sensors is that their pose (position and orientation) estimation error grows over time. This so-called drift can lead to false estimations such as passing through a wall. These false estimations could be corrected by using prior knowledge of the wall's location. In this work, I investigate *how* prior knowledge can be fused with inertial sensor measurements. The practical aim of this thesis is to eliminate the drift without additional sensors.

I investigate three types of prior knowledge regarding the environment and the movement: The human gait pattern, terrain maps, and event-domain maps. For all three types, I follow the concept of modeling the prior knowledge as probability distributions of the system's state. This modeling enables the usage of standard probability-based algorithms to estimate the position and orientation and to fuse the knowledge with sensor measurements.

The human gait is an alternating pattern of stance and swing phases. I show a new approach based on the Interacting Multiple Model Filter that can detect the phase and improve the velocity estimate of the inertial sensor. The approach automatically detects whether the sensor measurements match the probability distribution of the stance or swing phase. Simultaneously, it corrects the measurement errors of the inertial sensor by taking into account the probability distributions. The evaluation shows the potential of this method, albeit further development is required to outperform state of the art approaches.

Terrain maps define the height of a vehicle or a human given its position in the horizontal plane. This can be modeled as a so-called pseudo measurement. We act like there is a sensor that measures the height above the surface but always returns zero since there is no height difference. In this way, a probability distribution is modeled that constrains the position to the surface. I investigate terrain maps with the practical example of track cycling. I show that terrain maps can yield full observability of the position and orientation; in other words, that they are able to correct the growing error of the inertial sensor. Thereby, only the curved parts of the track yield information about the position. As a result, the position can be tracked during $10\,km$ drives with an error of $1.08\,m$ (RMSE).

Event-domain maps are a particular type of maps that specify where activities can be performed. For example, it is only possible to climb stairs at staircases. I investigate this type of knowledge at bouldering, where the climbers grip the holds of a route. The map represents a probability distribution of possible grip positions. I develop a two-step method where the first step estimates the transition between two holds. In a second step, the transitions are refined using the event-domain map. The estimated error improves from $0.266\,m$ (median) to $0.132\,m$ compared to an integrating solution without a map.

Overall, modeling the three types of prior knowledge successfully reduces the drift in all cases. The human gait pattern can be utilized with a new kind of state estimator, which needs

further investigation. The map-based types of knowledge correct the drift of the inertial sensor in the experiments. For the terrain map, it is even possible to prove the correction mathematically. This shows that prior knowledge modeled as prior distribution is effective to estimate the position solely with inertial sensors.

Zusammenfassung

Wie orten wir Menschen uns? Seit es das GPS gibt, ist es zur Gewohnheit geworden, dass wir immer und überall wissen wo wir sind und wie wir zu unserem Ziel kommen. Allerdings ist das GPS in Gebäuden blockiert. In der Wissenschaft wird nach geeigneten Technologien gesucht, um diese Lücke zu füllen. Ein Ansatz ist, genau wie wir Menschen, Vorwissen über unsere Umgebung und unsere Bewegung zu nutzen und mit Inertialsensoren zu kombinieren, da diese keine weitere Hardware in der Umgebung benötigen. Inertialsensoren weisen eine besondere Schwierigkeit auf: Man kann mit ihnen die Pose (die Kombination aus Position und Orientierung) berechnen, jedoch wächst der Fehler mit der Zeit immer weiter. Dadurch entstehen Abweichungen der Berechnung von der Realität, wie dass man durch eine Wand geht. Mithilfe des Vorwissens über die Position der Wände, kann man diese Fehleinschätzungen korrigieren. In dieser Arbeit untersuche ich, *wie* man Vorwissen effektiv zusammen mit Inertialsensoren nutzen kann. Dabei ist das praktische Ziel dieser Arbeit den wachsenden Fehler zu korrigieren.

Ich untersuche drei Arten von Vorwissen über die Bewegungsart und die Umgebung: Das Gangmuster des Menschen, Höhenkarten und sogenannte Aktivitäts-Domänenkarten. Für alle drei Vorwissensarten, folge ich dem Ansatz, Vorwissen als Wahrscheinlichkeitsverteilung zu modellieren. Dadurch kann man klassische wahrscheinlichkeitsbasierte Algorithmen zur Schätzung der Position und Orientierung nutzen und das Vorwissen mit den Messungen von Sensoren fusionieren.

Das Gangmuster des Menschen ist ein Wechsel aus Steh- und Schwingphasen. Ich zeige einen neuen Ansatz auf Basis des Interacting Multiple Model Filters, um diesen Wechsel zu erkennen und die Geschwindigkeitsschätzung zu verbessern. Der Ansatz erkennt automatisch, ob die aktuellen Messungen des Inertialsensors besser zur Wahrscheinlichkeitsverteilung der Steh- oder Schwingphase passen. Zeitgleich korrigiert er die Messfehler des Sensors indem er die vorgegebenen Verteilungen berücksichtigt. Die Auswertung zeigt das Potential der Methode; allerdings auch, dass noch weitere Entwicklung notwendig ist, um mit den etablierten Verfahren zu konkurrieren.

Höhenkarten legen für jede Position in der horizontalen Ebene die Höhe fest, auf der sich ein Fahrzeug oder ein Mensch bewegen kann. Dies lässt sich als eine sogenannte Pseudomessung modellieren. Es wird so gehandhabt, als gäbe es einen Sensor der die Höhe über der Oberfläche misst, jedoch immer 0 ausgibt. Dadurch modelliert man eine Verteilung mit hoher Wahrscheinlichkeit für Positionen nahe der Oberfläche. Ich untersuche dies am praktischen Beispiel des Bahnradfahrens. Ich zeige, dass die Höhenkarte volle Beobachtbarkeit der Pose ermöglicht, d.h., dass der wachsende Fehler des Inertialsensors korrigiert wird. Dabei gibt lediglich die gebogene Fläche der Bahnkurven Auskunft über die Position des Fahrrades. Beim Bahnradfahren lässt sich so die Position auf $1.08\,m$ (RMSE) bei $10\,km$ Fahrstrecke schätzen.

Aktions-Domänenkarten sind eine besondere Kartenart, die angibt wo Aktivitäten stattfinden können. So kann man beispielsweise nur auf Treppen Treppensteigen. Ich untersuche dieses Vorwissen anhand des Boulderns, bei dem die Kletterer an den Griffen einer Route greifen. Die

Karte lässt sich als Wahrscheinlichkeitsverteilung möglicher Greifpositionen interpretieren. Zur Positionsschätzung entwickle ich ein zweistufiges Verfahren, bei dem zunächst die Bewegung zwischen zwei Griffen geschätzt wird und diese dann mit der Karte der möglichen Greifpositionen korrigiert wird. Der Schätzfehler liegt bei $0.132\,m$ (Median) was eine deutliche Verbesserung gegenüber der kartenlosen Schätzung ($0.266\,m$) darstellt.

Insgesamt ist die Modellierung als Wahrscheinlichkeitsverteilung für alle drei Arten von Vorwissen erfolgreich. Für das Gangmuster des Menschen ergibt sich ein vielversprechender neuer Schätzansatz, welcher noch weitere Entwicklung benötigt. Beide kartenhaften Vorwissen führen in den Experimenten zur Korrektur des wachsenden Positionsfehlers des Inertialsensors. Für die Höhenkarte lässt sich dies analytisch belegen. Damit zeigt diese Arbeit, dass durch die Modellierung des Vorwissens als Wahrscheinlichkeitsverteilung die Pose allein mit Inertialsensoren geschätzt werden kann.

Contents

Acronyms **VIII**

List of Figures **IX**

List of Tables **IX**

1 Where are you? **1**
1.1 Localization with Prior Knowledge . . . 1
1.2 Contributions . . . 3

2 Fundamentals of State Estimation with Prior Knowledge **6**
2.1 Observability of States . . . 7
2.2 Standard Flat-Earth INS-Model . . . 8

3 Structural Characteristics of Prior Knowledge **10**
3.1 Unconditional DOF Prior Knowledge . . . 13
3.2 Conditional DOF Prior Knowledge . . . 14
3.3 Unconditional Domain Knowledge . . . 16
3.4 Conditional Domain Knowledge . . . 16
3.5 Observability Hierarchy of Prior Knowledge for MEMS INS . . . 17

4 The Human Gait as Prior Distribution **20**
4.1 Boxplus Interacting Multiple Model Smoother . . . 20
4.1.1 Boxplus Manifolds . . . 21
4.1.2 Manifold Reference Transform . . . 21
4.1.3 Boxplus-IMM-Smoothing . . . 22
4.1.4 Evaluation and Discussion . . . 23
4.2 Prior Modeling of the Gait . . . 24
4.3 Evaluation and Discussion . . . 24

5 Terrain Maps as Prior Distribution **27**
5.1 Track Cycling . . . 27
5.2 Observability Analysis . . . 28
5.3 Least-Squares Solution . . . 29
5.4 Dataset and Results . . . 30
5.5 Discussion . . . 31

6 Event-Domain Maps as Prior Distribution **33**
6.1 Bouldering . . . 33
6.2 Observability Analysis . . . 33
6.3 Divided-Estimation Solution . . . 34
6.4 Dataset and Results . . . 36

6.5 Discussion 37

7 Conclusion **38**

8 Future Work **39**

9 My Publications **A**

10 Literature **C**

11 Appendix **N**

11.1 Continuous Linear Input Dynamic Model of an INS . . . . . N

11.2 Full Observability Hierarchy for multiple Equations . . . . . N

Acronyms

ARMSE	Averaged RMSE
BOG	Bayesian Occupancy Grid
DOF	Degree of Freedom
EKF	Extended Kalman Filter
EKS	Extended Kalman Smoother
GNSS	Global Navigation Satellite System
GPS	Global Positioning System
HMM	Hidden Markov Model
IMM	Interacting Multiple Model Filter
IMMS	Interacting Multiple Model Smoother
IMU	Inertial Measurement Unit
INS	Inertial Navigation System
KF	Kalman Filter
LSTM	Long Short-Term Memory
MEKS	Multiplicative Extended Kalman Smoother
MEMS	Microelectromechanical System
MHE	Moving Horizon Estimator
MM	Multiple Model
OSM	Open Street Maps
PAC	Pedestrian Activity Classification
PDF	Probability Density Function
PDR	Pedestrian Dead Reckoning
PF	Particle Filter
RFID	Radio Frequency Identification
RMSE	Root Mean Square Error
RTS	Rauch-Tung-Striebel
SHS	Step and Heading System
SLAM	Simultaneous Localization and Mapping
UKF	Unscented Kalman Filter
ZUPT	Zero-Velocity Update

List of Figures

1 How humans could localize themselves by touch and their map of the environment. 2
2 The velocity of the human foot during gait as a multi-modal prior distribution. . . 3
3 The ambiguity of distance measurements. 7
4 Different modeling of the prior knowledge that cars drive on the street. 10
5 The difference of conditional and unconditional prior knowledge. 12
6 Observability hierarchy for INS. 18
7 Circular manifold with tangent space and a possible $\boxplus$-projection. 21
8 The same Gaussian expressed in two different tangent spaces. 22
9 Mean and covariance error of boxplus and naive mixing compared to optimal mixing over angular differences. 22
10 Comparison of $\boxplus$-algorithms (EKS, IMM, IMMS) and their reference algorithms. . 23
11 Comparison of the IMM approach with a state of the art detector. 25
12 The position estimate of the IMM approach compared against detector-based approaches for a single trial of the hallway dataset. 26
13 The track of the Sixdays Bremen. 27
14 Placements of the IMUs on the bike. 29
15 Trajectory of a biker in the first trial after 100 iterations of the optimizer. 31
16 Bouldering with inertial sensors at the hands, feet and hip. 34
17 Routes of the first climb wall in the study. 36

List of Tables

1 Prior knowledge structured by constraint type and validity. 12
2 Comparison of the IMM and IMMS approach against the LSTM classifier. 26
3 Results of the transition estimator, PF and PF smoother. 36

1 Where are you?

Where are you? A simple yet important question. One of the first questions in an emergency call. Answering it is not as simple as it may appear. In the past, humans used maps to locate themselves based on the landmarks they see [1]. Today, we can localize ourselves quickly using the Global Navigation Satellite System (GNSS), e.g., GPS. We can find each other based on our coordinates or navigate to our desired location.

Knowing your position precisely is not only relevant for navigation. Individuals can benefit from location-based services (LBS) such as location-based gaming or audio guides that always know which masterpiece a person looks at [2]. Unfortunately, GNSS do not work properly indoors since the satellite signal is blocked or deformed by the walls. Thus, answering where you are inside a building remains a significant challenge, even today.

Indoors, we have to replace the GNSS signal. Researchers are investigating extensively which technology can fill this gap. GNSS could be replaced by other sensor infrastructure, which is well suited for indoor environments. There are systems based on Bluetooth, Radio Frequency Identification (RFID) [3], ultrawideband [4] or flickering light bulbs [5]. These systems require additional sensor setups, which are expensive. Instead, Inertial Navigation Systems (INSs) can be used.

INS are based on Inertial Measurement Units (IMUs) that measure acceleration, angular rate, and often the magnetic field. The advantage of INSs is that most people already own the necessary hardware because IMUs are integrated into most smartphones [6]. The acceleration and angular rate measurements can be integrated to yield orientation, velocity, and ultimately, position of the sensor. Unfortunately, this process only yields suitable results for 1-2 min [6] since the built-in IMUs have low quality. While precise at short term, the errors of the IMU accumulate over time and grow infinitely, and thus, the estimate drifts apart from the true position. It is like walking with your eyes closed. The longer you walk, the more you lose your way.

1.1 Localization with Prior Knowledge

INSs are often modeled as if they could move freely in 3D space. Thus, the error of the estimate grows in all directions. But is it really true that an INS can move arbitrarily in space?
On the contrary, humans cannot move freely and we can use that to localize ourselves. With our eyes closed, we would bump into walls or furniture. While this is inconvenient, it actually helps us localizing ourselves (see Figure 1). Using our previously learned map, we can infer where the bump happened. We can also infer our position without bumping into the environment. If we did not touch anything, we walked a path without any obstacles. Thus, we can infer positional information from our map and motion. With similar procedures, the INS can benefit also from knowledge about the environment and dynamics.

The motion of humans has been extensively studied to reduce the IMU drift in Pedestrian Dead Reckoning (PDR). The regular human gait has an astonishingly constant step length [6] which can be used to correct the velocity drift. In so-called Step and Heading Systems (SHSs),

Figure 1: How humans could localize themselves by touch and their map of the environment. The human touches a chair, wherefore he can estimate his position in the map. Extracted from video at: `http://www.informatik.uni-bremen.de/agebv/zavi`

the steps and their heading are detected in the IMU data. The remaining position drift can be reduced with building maps [7]. Consecutive steps reduce the possible locations on the map since every trajectory crossing walls is impossible. The combined information from the gait pattern and building maps can yield a location accuracy of $0.73\,m$ [7].

The constraints on the possible motion of the IMU are not limited to PDR. Cars drive in the direction of their steering [8]. Usually, they are also constrained to stay on roads [9]. Similarly, ships [10] and aircraft [11] are bound to route corridors. The segments of a body are linked by joints [12]. Some type of constraint that contains knowledge about the system appears in almost any application.

To correct the position drift of an INS, knowledge of the position is required since even the best velocity estimation has minor errors that accumulate over time. In the literature, maps are the most common source of position information. Building [7, 13–16] and route maps [9, 17–21] are widely used as constraints on the position. Furthermore, terrain maps that contain the height of the terrain [1, 22–24] and event-domain maps that match activities to locations [25] can be used to improve the position estimate.

Prior knowledge can be used as a probability distribution of the state, the so-called prior distribution. The prior distribution contains the probability of each possible state, e.g., the position, without using any measurement. For example, a building map is a prior distribution where all positions inside the walls have zero probability. This concept has the advantage that probabilistic state estimation algorithms can be used to optimally fuse knowledge with measurements. Furthermore, the imprecision and uncertainty of the knowledge can be considered. It can be modeled that vehicles can have a slight drift instead of driving forward [8] or that the foot is not entirely at rest due to detection errors [26]. Although this concept is applicable to a wide range of prior knowledge, ad-hoc solutions are often used.

In my thesis, I investigate three types of prior knowledge from the literature using the concept of prior knowledge as prior distribution. My practical aim is to correct the drift of INSs without additional sensors. It lies in the nature of prior knowledge that it is specific for applications, and thus, ad-hoc solutions are used to apply prior knowledge. Instead, using prior knowledge as prior distributions enables top-level investigation on algorithms to optimally fuse different kinds

of distributions with measurements [27–30]. Applications with the same knowledge structure can benefit from any improvement achieved on the algorithmic side. Therefore, my methodical goal is to generalize knowledge from the literature as prior distributions so that its usable in probabilistic state estimation.

1.2 Contributions

I show that the human gait pattern can be modeled as a prior distribution to improve the velocity estimate. The gait pattern can be separated into stance and swing phases. The foot rests on the ground with zero velocity during the stance, whereas the velocity is nonzero during the swing. In the PDR approach, the stance phase is detected and the velocity is updated with a prior distribution close to zero, the so-called Zero-Velocity Update (ZUPT) [26]. However, not only the stance phase may be assigned a prior distribution. In the swing phase, the foot accelerates and decelerates back to zero velocity. Thus, the velocity is distributed more broadly, but still close to zero (see Figure 2). Overall, this kind of distribution is multi-modal, i.e., the system has multiple modes and each mode has its own prior distribution.

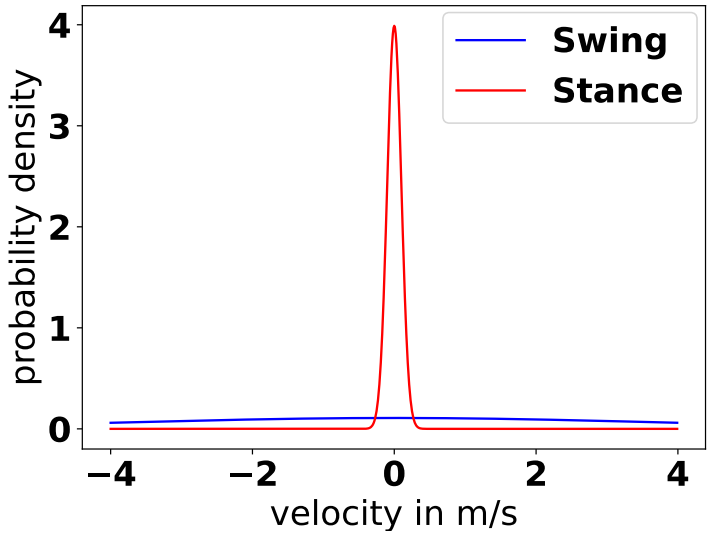

Figure 2: The velocity of the human foot during gait as a multi-modal prior distribution.

Multi-modal distributions can be estimated with the well known Interacting Multiple Model Filter (IMM). I apply the IMM to the human gait instead of using the ZUPT. I show that this approach can estimate the gait phase and velocity simultaneously. The standard IMM is not applicable to estimate the orientation of a system since it cannot handle the mathematical properties of orientations. Thus, I first develop a generalization of the IMM for manifold states. Furthermore, I develop an Extended Kalman Smoother (EKS) and Interacting Multiple Model Smoother (IMMS) on manifolds to smooth the estimation. As a proof of concept, I evaluate my IMM approach on a real-world dataset.

I show that terrain maps can be used in their basic form, i.e., as a prior distribution of the position, to correct the INS's position drift. Terrain maps give a relation between the position in

the plane and the height. Ground vehicles are bound to drive on a surface, which constrains not only the position but also their velocity and orientation. In [1, 31], the trajectory's slope is matched to an inclination map instead of the terrain map and in [22, 23], a barometer measures the height. Neither a barometer nor the conversion to an inclination map is necessary. I record a real-world dataset and show experimentally that the INS drift is corrected with the terrain map. Furthermore, I prove mathematically that the track's terrain map yields full observability. To the best of my knowledge, this is the first formal observability proof for terrain maps with INS.

I investigate how the unique event-domain maps can be modeled as a prior distribution. Fundamentally, we expect map knowledge to be unconditionally valid since the map describes the static environment. In some cases, we can retrieve our position in the map from certain events. For example, it is possible to detect when a pedestrian opens a door, drives an elevator, or takes the stairs [25]. These actions require infrastructure in the environment. Maps of these infrastructures are used in Pedestrian Activity Classification (PAC) to aid position tracking. The challenge is that the same event can occur at different positions. To find the correct event location, at first, the events are detected. The walked distance and direction between locations, i.e., the transition, is estimated and matched to possible transitions in the map. The matching is conducted by a Hidden Markov Model (HMM) and the Viterbi algorithm [25]. The map transition is then used to estimate gait parameters like the step length.

The HMM approach to event-domain maps is elegant, but models the event locations as single points instead of a prior distribution. It neglects that the event does not necessarily takes place exactly at the event location. Instead, I develop an approach based on the Particle Filter (PF) [32] that can perform the map matching implicitly. The PF can account for different prior distributions, wherefore the method is a generalization. I record a real-world dataset with 27 participants and evaluate my approach.

Overall, my publications[1] show how various types of knowledge can be used as prior distributions. All my publications build upon probabilistic state estimation methods. Thus, my approaches can be transferred to other applications with knowledge of the same type. I show, in practical applications, that the knowledge is capable of correcting the INS drift.

The remainder of this thesis is structured as follows: I start with fundamentals of state estimation with prior knowledge in Section 2. I show how prior knowledge is used as prior distributions and which type of knowledge is considered in this thesis specifically. I introduce the concept of observability and also show the standard INS model which is the basis for all my works.

In Section 3, I classify different types of prior knowledge based on their mathematical modeling. I summarize example applications of the four classes of prior knowledge I identified. I retrieve the hierarchic observability tree for INS with Degree of Freedom (DOF) knowledge. It can be used to lookup whether a chosen prior knowledge can yield observability of the states.

I continue with the modeling of the human gait as a prior distribution in Section 4. It starts with the generalization of the IMM for manifolds. The generalized IMM is used in a proof of concept to show, that the human gait can be modeled as the prior distribution shown in Figure 2.

In Section 5, I investigate 3D terrain maps with track cycling as the example application.

[1] My publications are cited with roman numerals, e.g., [IV].

I the review experimental and mathematical proof that the bike's position and orientation are observable through the prior knowledge.

I show my methodology to apply event-domain maps with ambiguity and the results on a newly recorded dataset in Section 6. I use bouldering as an example application to show the correction of the INS's drift.

In the end, I summarize my work and show possible future directions.

2 Fundamentals of State Estimation with Prior Knowledge

In state estimation, sensor measurements are fused using imperfect measurement models. Furthermore, the measurements are disturbed by random noise. Therefore, it is not possible to achieve a perfect state estimate. Instead, the Probability Density Function (PDF) $p(x_k)$, which represents the uncertainty of the system's current state, is estimated [33].

The uncertainty can be reduced with the measurements z_k in the so-called update step. We apply the Bayes theorem, which enables us to correct the PDF based on the sensor's physical principle, the so-called measurement model h. The Bayes theorem simplifies state estimation because it automatically calculates the corrected state probabilities based on the measurement model, even for indirectly measured states. The measurement model is used to compute the measurement probability $p(z_k|x_k)$ given the system's current state. It is multiplied with the prior distribution $p(x_k)$ to compute the updated state PDF $p(x_k|z_k)$:

$$p(x_k|z_k) \propto p(z_k|x_k) \cdot p(x_k) \tag{1}$$

The system's state can change between measurements. In order to account for this, a model of the state change is required, which is called the dynamic model. It defines how the system evolves over time given the dynamic input u_k, e.g., the acceleration. In the case of INS, the dynamic model integrates the measured angular rate and acceleration to orientation, velocity and position.

With the dynamic model, the transition probability $p(x_{k+1}|x_k, u_k)$, i.e., the probability to move to a new state x_{k+1} given the old state x_k, can be computed. The transition probability is multiplied with the measurement-corrected PDF:

$$p(x_{k+1}|u_k, z_k) \propto \int p(x_{k+1}|x_k, u_k) p(x_k|z_k) dx_k \tag{2}$$

This step is called prediction because it predicts the PDF at the next time step. Errors flaw the dynamic model and dynamic inputs, wherefore the prediction increases the uncertainty of the estimate. However, it allows connecting the measurements from different time steps.

The prediction and update steps can be performed alternatingly to fuse consecutive measurements. The computed probability distribution $p(x_{k+1}|z_k, u_k)$ is used as the prior distribution $p(x_k)$ of the next time step.

My goal is to reduce the uncertainty of the state estimate with prior knowledge. The knowledge can be applied at different points of the state estimation. I focus on knowledge about the state itself, meaning the dynamic probability $p(x_{k+1}|x_k, u_k)$ but mainly the prior distribution $p(x_k)$. In principle, this knowledge can be either used as the prior distribution $p(x_k)$ or to create a prior distribution with higher certainty by combining the estimated pdf with the knowledge $p'(x_{k+1})$ to a new prior distribution:

$$p(x_{k+1}) \propto p'(x_{k+1}) \cdot p(x_{k+1}|z_k, u_k) \tag{3}$$

The creation of the combined prior distribution is a multiplication of two probability distributions,

just like in the update equation (1). Thus, it is often possible to use prior knowledge like a measurement - a so-called pseudo measurement [27, 29, 34].

In certain applications knowledge is used to improve the error models of the sensors. For example, in radar tracking [35], terrain maps are used to identify challenging locations for the measurements, such as locations where the signal is disturbed by echoes. Such knowledge affects the measurement distribution $p(z_k|x_k)$. I do not consider it in my thesis since it is applied differently than prior knowledge of the state.

2.1 Observability of States

The state estimation uncertainty is counterbalanced by the prediction and update step. Since the measurements are imperfect, a single measurement cannot fully correct the uncertainty of the state estimate [36]. The uncertainty reduction depends on the certainty of the measurement and the current certainty of the state estimation. The higher the certainty of the state estimate compared to the measurement, the less the certainty is corrected.

In INSs without additional sensors, the measurements do not carry sufficient information to balance the uncertainty introduced by the dynamics. The magnetometer measurement can only correct the pose uncertainty which stems from the heading error but not from the acceleration error. Thus, the uncertainties of the velocity and the position grow endlessly.

The growing error of INS is the reason to combine INS with additional sensors. However, not all sensors are suited to correct the drift as their measurements may contain ambiguities [37]. For example, distance measurements to a single beacon cannot uniquely determine the rotation around the beacon (see Figure 3).

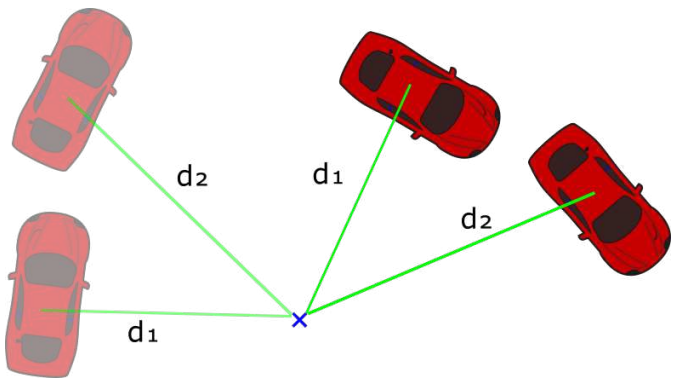

Figure 3: The ambiguity of distance measurements. The distance between a beacon and a driving vehicle is measured (d_1, d_2). A trajectory of the vehicle that is rotated around the beacon yields the same distance measurements (faded version).

Whether or not a set of sensors can correct the growing error can be analyzed using the concept of observability [37, 38]. A state is observable if it can be unambiguously determined given a measurement series knowing the starting region[2]. Intuitively, a state is not observable

[2]Technically, this is local observability. A globally observable state can be unambiguously determined from the measurement series without knowing the starting region.

if it can change while the measurements z_k and the dynamic inputs u_k stay constant. The measurement errors are ignored in the observability analysis since it is not possible to determine the state unambiguously with noise. Nevertheless, it is relevant for real applications since the state cannot be estimated in the long term with noise if it is not possible without noise.

The observability of nonlinear systems can be analyzed via the Jacobian rank test [38] or the rank observability criteria [39]. Both observability tests build upon the inverse function theorem [40]. The measurements are a function of the full state. The inverse of this function would compute the states based on the measurements, which is the overall goal of state estimation. Thus, if the inverse does not exist, the state cannot be estimated. The inverse function theorem simplifies the search for the inverse function. It states that the local inverse exists and only exists if the Jacobian of the measurement equation with respect to the state is invertible. Therefore, both observability tests check for the invertibility of the Jacobian.

The Jacobian rank test uses the time derivatives of the measurements to model a whole series of measurements. Likewise, the rank observability criteria uses Lie derivatives [39]. The advantage of the rank observability criterion is that it can run automatically and prove unobservability, whereas the Jacobian rank test can only prove unobservability if infinite derivations of the measurement equation are considered. However, the definition of the rank observability criterion is slightly more ambiguous because it requires sufficient excitation of all DOF of the system, e.g., acceleration in the x-axis alone may be insufficient to observe the state. This is a drawback for prior knowledge since DOF constraints specifically block certain DOFs that cannot be excitated. Thus, it may be possible that a sensor measurement would yield observability but not the pseudo measurement.

2.2 Standard Flat-Earth INS-Model

Throughout this thesis, I use INS that share a common state and dynamic model. For this reason, I briefly present the standard system description.

INSs are deployed to estimate a moving object's orientation, velocity and position. They consist of an accelerometer, a gyrometer, and a magnetometer combined in an IMU and are often combined with sensors like GNSS [41] or cameras [42]. The continuous state space X_c [43] of an INS consists of the position $\vec{p}_W$, the velocity $\vec{v}_W$ and orientation q_W^I in world coordinates as these are the states of interest. Furthermore, the continuous state contains the biases of the accelerometer b_a, the gyrometer b_g and the magnetometer b_m. These are disturbances of the measurements that manifest as offsets. Thus, a state x_k at time k is represented as:

$$x_k = \begin{pmatrix} q_W^I & \vec{p}_W & \vec{v}_W & \vec{b}_a & \vec{b}_g & \vec{b}_m \end{pmatrix}^T \tag{4}$$

This so-called flat-earth model ignores the Earth's surface curvature, the Earth's rotation and assumes constant gravity [44]. My applications stay in one building, wherefore the curvature and gravity change can be neglected. Furthermore, I use low-cost Microelectromechanical System (MEMS) IMUs, which are too imprecise to measure the Earth's rotation [45].

The system moves over time, and thus, the state changes. The movement is estimated by integrating the measured acceleration $\vec{a}_I$ and angular rate $\vec{\omega}_I$ measurements to orientation, velocity and ultimately to position. This is captured in the dynamic model $g : X \times U \mapsto X$.

$$g(x, \vec{a}_I, \vec{\omega}_I) = \begin{pmatrix} q_W^I * \exp\left(\frac{(\vec{\omega}_I - b_g)\cdot\Delta T}{2}\right) \\ \vec{p}_W + \Delta T \vec{v}_W + 0.5\Delta T^2 \vec{a}_W \\ \vec{v}_W + \Delta T \vec{a}_W \\ (1 - \frac{\Delta T}{\tau_a})\vec{b}_a \\ (1 - \frac{\Delta T}{\tau_g})\vec{b}_g \\ (1 - \frac{\Delta T}{\tau_m})\vec{b}_m \end{pmatrix} \boxplus \varepsilon_g, \quad a_W = q_W^I * (\vec{a}_I - \vec{b}_a) * \overline{q}_W^I + \vec{g}, \tag{5}$$

The acceleration and angular rate measurements are corrected with the biases. The $\exp(\cdots)$ function [46] creates a quaternion that rotates the orientation according to the corrected angular rate. The corrected acceleration is rotated into world coordinates where the gravitation $\vec{g}$ is corrected. The biases are modeled as random walks with a constant decorrelation time τ_i [47]. In short experiments, the biases are modeled as constants because they usually change slowly. $\varepsilon_g \sim \mathcal{N}(\vec{0}, \Sigma_g)$ is the random error of this model compared to the true dynamics. It is applied with the $\boxplus$-operator (pronounced boxplus) [46], which is required since the orientation is no vector quantity. I will go into more detail on the $\boxplus$-operator in Section 4.1.1.

The magnetometer measures the local magnetic field $\vec{m}_W(\vec{p}_W, t)$ in sensor coordinates:

$$m(x,t) = \overline{q}_W^I * (\vec{m}_W(\vec{p}, t)) * q_W^I + \vec{b}_m + \varepsilon_m, \tag{6}$$

where $\varepsilon_m \sim \mathcal{N}(\vec{0}, \Sigma_m)$ is the random error of the magnetometer.

Depending on the application, additional physical properties are added to the continuous state of the INS. Furthermore, in some applications, behavioral properties of the system like `is walking`, `is standing` or `is gripping` are relevant. Using the notion of hybrid estimation, these behavioral properties — also called system's mode — can be modeled as the discrete state space X_d [43]. The discrete state space is only represented with natural numbers $\mathbb{N}$.

3 Structural Characteristics of Prior Knowledge

Prior knowledge exists in many forms and shapes. Astonishingly, various types of prior knowledge can be used with the same estimation algorithm since it constrains the state with the same type of prior distribution. Thus, the knowledge can be characterized by its distribution type [27, 30]. A challenge is that the identical prior knowledge can be modeled differently so that it applies different distributions. However, this enables us to explain all types of distribution models with a single example.

Let us try to model that a car drives on a street (see Figure 4). In a first attempt, we could assume that the car always drives at the lane's center (or that the lane has zero width). As a result, the three position directions would be interdependent and could be computed from the traveled distance along the road. This is called an equality constraint since we can find an equality function.

Drivers are probably not capable of holding the car at the center exactly. Hence, we could allow small deviations from the center position while the overall motion stays on it. The result is a soft version of the equality constraint.

While it may be true that the cars are, on average, around the lane center, some drivers may tend to drive on the left or right side. Thus, we can only say certainly, that the cars stay on the lane. We can model this as an inequality that states that the car's position is always right of the left border and left of the right border. Hence, we call it an inequality constraint. Positions, where even one wheel is outside the street, would be neglected.

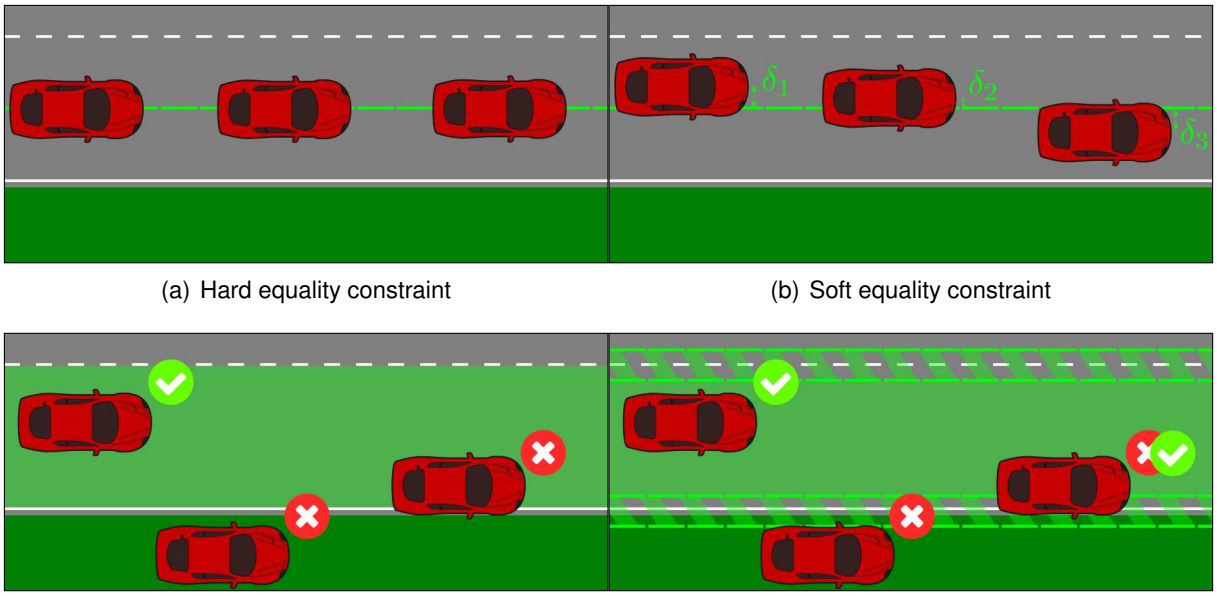

(a) Hard equality constraint (b) Soft equality constraint

(c) Hard inequality constraint (d) Soft inequality constraint

Figure 4: The prior knowledge that cars drive on the street can be modeled diversely. It can be assumed that the car stays at the center of the road (a). Small deviations δ_i towards the road center can be allowed (b). The car can be allowed to be anywhere between the road borders (c). The borders may be known imperfect (d).

Although it is reasonable to assume that the cars stay inside the borders, this modeling may neglect the true position of the car. The reason is that we do not know the position of the street's borders exactly. We can model this as a soft inequality constraint where the borders are assumed to have an error [29]. Some positions are clearly on- or off-road, but positions close to the border are indeterminate.

Prior knowledge usually applies soft constraints to the system. As [15] pointed out, there is often some degree of uncertainty in prior knowledge. While the semantic information may seem absolute, the numeric information cannot be obtained perfectly since it must be measured. Nevertheless, hard constraints occur in mathematical structures like rotation quaternions [48] or due to fundamental physical laws like the conservation of angular momentum [49].

Equality constraints constrain the DOF of the state space. The state can only change in a specific direction, e.g., the car can only drive in the direction of the lane. Thus, I refer to them as DOF knowledge. DOF knowledge can be modeled as a prior distribution like:

$$p'(x) = \mathcal{N}(m_d(x); 0, \Sigma_d) \tag{7}$$

where $m_d(x)$ is the constraint function.

Soft inequality constraints are rarely shown in the literature. In [29], states outside the boundaries receive a probability based on the frequency of constraint violations in the ground truth. The softness of the constraint can stem from the inaccuracy in measuring the bounds. [15]. A possible solution is two model the inaccuracy with Gaussians and to integrate over all possible bounds. Apart from these works, only hard inequality constraints are used in the literature.

Hard inequality constraints can be modeled as:

$$p'(x) = \begin{cases} f(x), & \text{if } m_r(x) <= B_r \\ 0, & \text{else} \end{cases}, \tag{8}$$

where $m_r(x)$ is a mapping function, B_r are the bounds of the constrained region and $f(x) > 0$. $f(x)$ can be any probability distribution but is often chosen to be uniform. I call this type domain knowledge since the prior distribution may allow a state domain that consists of multiple regions. Each of these regions is defined by an inequality constraint.

In addition to its type, I categorize prior knowledge based on its validity. Let us think again about cars driving on streets. We can assume that the cars stay at their lane. However, during overtaking, they may leave it (see Figure 5). Thus, we would have to check that the car is not overtaking to apply the knowledge. We may assume that certain knowledge is unconditionally valid for some applications, e.g., a car is always on the lane if overtaking is forbidden.

The prior distribution of conditional knowledge is uniform if the condition is not met:

$$p'(x) = \begin{cases} f(x), & \text{if } \texttt{condition} \\ c, & \text{else} \end{cases}, \tag{9}$$

where c is a constant so that the integral of the prior distribution is 1.

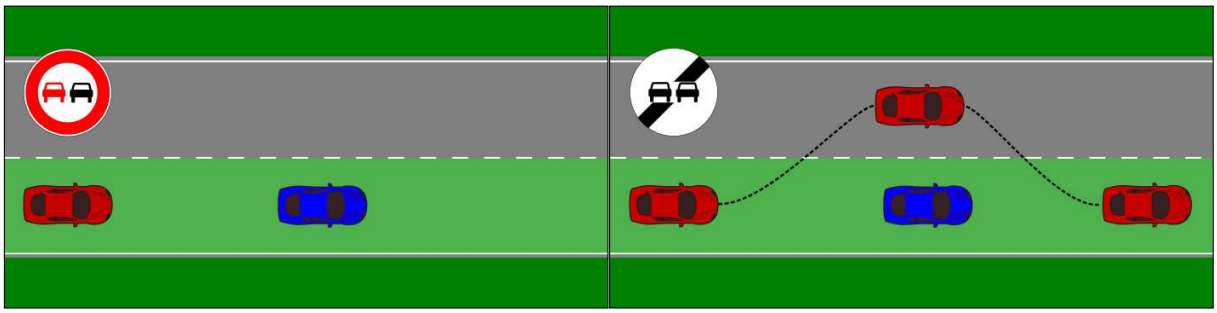

(a) Unconditional constraint (b) Conditional constraint

Figure 5: Cars only stay in their lane if they do not overtake others. Overtaking may be prohibited (a) or allowed so that the car can be at the opposite lane (b).

In summary, prior knowledge can be classified based on two properties of its model:

1. The type of the constraint (DOF or domain)
2. The validity of the constraint (conditional or unconditional)

The properties influence the choice of algorithms to deploy prior knowledge in state estimation and the analysis of the system's observability. With these considerations in mind, I structure various kinds of prior knowledge from the literature into four classes, as shown in Table 1. In the next sections, I shortly present examples of prior knowledge from the four categories, which observability tests are applicable and which algorithms are used.

Table 1: Prior knowledge structured by constraint type and validity.

Type	DOF constraint		Domain constraint	
Unconditional	Route map	[50–53]	Traversal maps	[7, 13–16, 54]
	Known destination	[55, 56]	Traversal map SLAM	[57]
	Link connections	[12, 58–63]	Max acceleration/velocity	[11]
	Vehicle constraint	[8, 64, 65]	Route width	[29, 66]
	Underwater dynamics	[67]	Corridor heading	[68]
	Terrain maps	[1, 22–24, 31]	Maximum distance	[69, 70]
	Low acceleration	[59, 71]		
	Constant position/slope	[59, 65]		
	Border avoidance	[72]		
Conditional	Route maps	[9, 17–21, 73]	Event landmarks	[25, 74–77]
	Gait cycle	[26, 78–80]	Event landmark SLAM	[81–83]
	Stationary updates	[60, 84, 85]		
	Freefall dynamics	[86]		
	Multiple dynamics	[10, 17, 87–89]		
	Floor properties	[90]		
	Minimum distance	[91]		
	Wall contact	[92]		
	Vertical acceleration	[93]		
	Corridor heading	[94]		

3.1 Unconditional DOF Prior Knowledge

The non-holonomic vehicle constraint of [8] is a widely used unconditional DOF prior knowledge, even in systems without an IMU. Wheeled vehicles can only drive forward wherefore their velocity and orientation are dependent. This is often modeled as zero velocity in the lateral directions. It has been shown that this prior yields observability of the IMU biases, the body velocity, and the inclination if the vehicle drives a curve [95, 96]. This stems from the centrifugal force that relates acceleration with velocity and angular rate. On flat ground, vehicles also have low acceleration in the z-direction and mainly change their heading [65]. Other vehicle types, like underwater vehicles, have their own specific dynamics that can be exploited as prior knowledge [67].

Orientation estimators use the accelerometer to measure the direction of gravity. It is often assumed that the accelerometer measures only gravity [71]. It has been pointed out that this is an assumption of low acceleration [59].

Not only the acceleration can be low, but also the position change, e.g., when walking in a room [59]. On flat grounds, vehicles have a constant height, and on streets, the slope usually changes gradually [65].

The segments of the human body are connected via joints. Thus, IMUs on two connected segments measure the same acceleration and angular rate except for the lever arm and the joint rotation. The acceleration [12] and velocity [97] at the joint can be estimated by each IMU separately, but must be equal. This is used as an equality constraint and allows to measure each segment's inclination and relative heading. By placing IMUs at each segment, the complete body posture can be estimated. This knowledge applies to any joint-connected segments, such as sway cranes [62].

It is not strictly necessary to place the IMUs at every segment. The relative orientation of three segments connected by two nonparallel hinge joints can be estimated with only two IMUs if the motion excites all DOF [98]. In [61], statistical models of the joint motions are used to estimate the complete body posture with only 6 instead of 17 IMUs.

In [53], the flight route information is used to model the expected dynamic behavior. Furthermore, route information can be used as knowledge about the position. A train rail constrains the train onto a curve in the 3D space [52]. Cars are constrained to stay on the road [50]. Building maps can be simplified to route maps by assuming a small corridor width [51]. Not only the full route map but also the destination of the trajectory can be used, since it defines the overall dynamics of the system [55, 56].

More complex route information in the form of terrain maps can also improve the estimation results. A barometer's height measurement [22, 23] or height difference measurement [24] can be fused with the terrain map to find the position. In [1, 31], an inclination map is combined with an IMU as the only sensor to correct the INS drift.

Although map borders are usually domain knowledge, they can be used to constrain the DOF of the dynamic model [72]. Crewed vehicles do not violate map borders to avoid crashes. Thus, the dynamic behavior contains information about the relative position to a border.

The observability with DOF knowledge can be tested by standard observability tests, e.g., the Jacobian rank test [38] or the rank observability criterion [39]. The equality constraint function can be seen as a perfect or pseudo measurement [27, 34]. The idea is to act as if a sensor exists, which measures the constraint's error, e.g., the distance to the route. Since we assume that the constraint always holds, the distance is always zero. Thus, no real sensor is needed. With the pseudo measurement equation, the observability can be tested.

The usage of equality constraints in state estimation has been extensively studied [27, 28, 30]. Several approaches exist to incorporate the constraint. One approach is to incorporate the constraint into the system's model by model reduction. This approach is mainly suited for hard knowledge or soft knowledge with only little variance since no constraint violation can be modeled. Another possibility is to project the state estimate and the process noise on the constrained surface. It is also applicable to soft constraints by projecting only into the direction of the constraint.

In this thesis, I use the pseudo measurement method, which is also used for the observability analysis. The constraint is introduced into the system as a measurement. This allows to universally use constraints in unmodified state estimators that can use measurements, e.g., Gaussian estimators such as the Extended Kalman Filter (EKF), Unscented Kalman Filter (UKF) or least-squares estimators. The main drawback of the method is that the errors of pseudo measurements are correlated, wherefore a bias is introduced into most estimators.

3.2 Conditional DOF Prior Knowledge

Systems often repeatedly go into stationary modes. In these, the systems have zero velocity and zero angular rate. Stationary updates of the angular rate yield the gyrometer biases observable and the accelerometer bias can get observable if the INS rotates between ZUPTs [99]. The body velocity can be observed from the ZUPT, but the heading, and thus, the world velocity is unobservable. Stationary updates can even be used to calibrate IMU parameters if nine distinct attitudes are used [100].

During the stance phase of the human gait, i.e., when the foot is on the ground, the ZUPT is used with foot-mounted IMUs [85]. This reduces the cubic integration error of the IMU to a linear error. Errors of less than 2% of the traveled distance are reported [60]. In [90], the floor type influences the gait so that optimized stance detectors for the different dynamic behaviors can be used. It has been pointed out that the foot is not completely stationary wherefore step lengths are often underestimated [26].

With two foot mounted IMUs additional constraints can be used. In [91], it is stated that the feet have a minimum distance during walking. They achieve this distance when the swinging foot passes the standing foot. This moment can be detected and used as a minimum distance update.

Another way to use the gait dynamics is to count steps. In SHS, steps and their heading are detected and the position is advanced by the step length [3, 78, 79]. The almost constant step length of pedestrians is utilized here [6]. Despite the two-phase gait model with *stance* and

swing, a four-phase model with *heel-strike* and *push-off* can be used to distinguish different types of walking like upstairs, downstairs or level walking [80].

Stationary updates can correct the heading as well. In buildings, the heading stays close to the cardinal direction of the building since people follow the corridors [94]. Turning motions have to be detected so that the movement direction can change.

In addition to the stationary updates, free fall dynamics can be used. In jump height estimation, the knowledge is used that jumping humans are essentially in free fall with a starting velocity. The jump height is computed based on the free fall time [86].

In [93], the IMU is placed on a bicycle's crank. The measured acceleration is maximal or minimal if the gravitation and the centripetal acceleration are aligned, i.e., when the crank points up- or downwards. These moments are detected and used to update the crank angle.

Prior knowledge is not only useful for indoor tracking where the GNSS is generally blocked but also for outdoor purposes where the GNSS is temporarily unavailable or disturbed by multipathing or weather conditions. In these cases, pose estimation can be supported via route maps. The maps can be used for direct curve matching via HMMs [19] or as position constraints [21, 73]. While driving on the road could be modeled as unconditional knowledge, it is modeled conditionally in practice. The reason is that multiple routes are possible at junctions and the correct lane has to be extracted. This can be supported using multiple dynamic models that model either *keep lane* or *change lane* [17, 20]. In [18], the road is divided into short straight segments, and a Gaussian model for each segment is used.

Multiple dynamic behaviors of a system can be seen as a kind of conditional DOF knowledge of the system. Usually, these are used in systems with unknown dynamic inputs, where the dynamic behavior can be extracted from sensor measurements. Ships perform specific maneuvers to drive on a route or to change it [10], different flight dynamics can be used to improve radar aircraft tracking [88] and even different kinds of physical contact cause different dynamic behavior [89]. Nevertheless, INS can be supported with this knowledge [87].

Usually, crashes with the environment are avoided by any system. In contrast, the rollocopter in [92] maps the environment by crashing into it. Depending on the crash velocity and angle, the rollocopter bounces off the environment with a computable acceleration and angular rate. Even this knowledge can be used to improve the position estimate.

In general, the observability of conditional DOF knowledge can be analyzed like unconditional knowledge. In the interpretation, the validity has to be considered. The state is only observable at the times when the knowledge is valid.

Likewise, conditional DOF knowledge is used in state estimation like unconditional DOF knowledge. The only difference is that a detector is needed to detect when the knowledge is valid. Since the dynamic behavior also depends on the mode of the system, Multiple Model (MM)-estimation techniques can be used [101]. The most popular is the IMM, which can reduce the ever-growing number of possible mode sequences to a limited number of Gaussian distributions [88, 102, 103]. The estimation quality can be improved by adaptively changing the set of active modes in a variable structure IMM [9, 104]. If the models require different state descriptions, the mixing introduced by [103] can be used to prevent state bias.

3.3 Unconditional Domain Knowledge

Domain knowledge can be as simple as bounds on the state. For example, the acceleration and velocity of an object are limited, which can be used to bound the velocity drift [11].

Feet are connected by the legs and hip [69, 70]. Thus, the pose estimation can be improved by using two foot-mounted IMUs and constraining their maximum distance.

The aforementioned heading correction can be used as unconditional domain knowledge as well. The cardinal heading directions of buildings have a higher prior probability than other directions [68]. With this modeling, short direction changes are possible while long-term walks are drawn towards the cardinal directions.

Bounds on the position can be much more complicated. In the simplest case, the route's width truncates the domain [29], but the width can also depend on the longitudinal position on the route [66]. The complexity can rise to traversal maps that define all traversable positions, e.g., road maps [13] or building maps [14–16]. Even detailed maps like Open Street Maps (OSM), which contain the street type, elevation and obstacles like trees are used [54]. With sufficient motion, a traversal map allows localizing inside a building [7]. It is also possible to map the environment with a foot-mounted IMU alone since humans adapt their behavior to the walls [57].

The observability of complex domain prior knowledge cannot be analyzed directly with the known tools. Narrow boundaries may be modeled as equality constraints. In this case, the knowledge can be analyzed with the observability tests for DOF knowledge. In contrast, complex, multi-modal traversal maps can hardly be modeled as equality constraints. Without a measurement equation, the tests cannot be applied.

The simple case of state boundaries can be incorporated into Gaussian estimators like the Kalman Filter (KF). The constraint can be incorporated so that no action is taken when the estimate does not violate the inequality. If it is violated, it is handled like an equality constraint on the boundary [28]. Other possibilities are to truncate the Gaussian [28, 69] or to project it into the allowed region via inequality-constrained least-squares optimization [70].

Due to the multi-modality, traversal maps are used with PFs [7, 14–16]. The PF has the advantage that it can represent multimodal distributions with the particles, and that constraints can be applied via importance sampling [29, 32]. The PF is used due to its simplicity, but can fail if all particles violate the constraint [105]. As a workaround, the knowledge can be applied in the prediction step by resampling predicted particles until they comply with the constraint. In return, the computation time can grow infinitely [29].

3.4 Conditional Domain Knowledge

Conditional domain knowledge is rare in the literature. The only used type of knowledge is the knowledge of event landmarks or rather event domains. These are positions where specific activities, such as turning, opening doors or walking stairs, take place [74, 75]. The events are detectable in the IMU data, but multiple positions on the map may correspond to the same event. Thus, the constraint is multi-modal.

The observability of conditional domain knowledge cannot be analyzed with the standard tests just like the unconditional domain knowledge. Again, sufficiently narrow domains may be modeled as an equality to analyze the observability. However, that is not possible in the case of event-domain maps. Since multiple domains correspond to the same event, the true event-position, which is required for a pseudo measurement, is unknown.

Although conditional domain knowledge applies an inequality constraint on the state, it is used differently in the literature. If the positions of the landmarks are known, e.g., from the building maps, the most common technique is map matching [74, 76, 77]. An SHS approximates the position transitions between two events and the probability for each possible location transition is calculated. The Viterbi algorithm can extract the true position sequence [25].

Apart from map matching, the event landmarks can be effectively used as loop closures in pedestrian SLAM [82, 83]. The output map contains the locations of the landmarks, which indicates the room structure. In combination with crowd-sourcing, the landmarks' positions can be estimated with an accuracy of 0.8-1.5 m [81].

3.5 Observability Hierarchy of Prior Knowledge for MEMS INS

The observability of a system can be tested based on the measurement equations and the dynamic model. A state is not observable if it can change without changing the measurements. Thus, a state is not observable if it does not occur in the system's measurement equations.

More measurement equations can be generated by differentiation [38]. Technically this means to use a series of measurements to observe a state rather than a single measurement. By derivation, other states can occur in the measurement equation. For example, in an INS, the derivative of the position is the velocity. Depending on the dynamic model, further states occur with further derivations. Therefore, a hierarchy of states exists. This hierarchy gives a minimum requirement for observability of states: Either the state itself or an antiderivative state have to occur in the measurement equation.

Such a hierarchy is helpful for prior knowledge as it can give us a first impression of the observability without further proof. However, observability is not only about occurrence in the equation. A state may be unobservable due to symmetries, where another state, which can have the same effect on the measurement, conceals the change. Thus, an observability hierarchy based on occurence only is too simple. Instead, I derived an observability hierarchy based on automated observability tests.

The rank observability criterion can automatically check the observability of a system [39]. Furthermore, it can be used to check the observability state-wise as described in [37]. The criterion requires the time-continuous dynamic model in the linear input form (see Appendix 11.1) and the measurement equation.

I tested the observability of an INS with all kinds of measurement equations of pure states, e.g., a direct measurement of the heading. In addition to single state measurements, I tested common knowledge about the velocity. The resulting hierarchy effectively gives the minimum requirement for observability of each state (see Figure 6).

Note that the hierarchy is still a minimum requirement, although it is based on an observability test. The rank observability criterion does require sufficient motion to achieve observability. The prior knowledge can specifically block the required motion. Consider a car driving on a horizontal plane. The velocity in the z-axis would be constant which may yield information about the accelerometer biases. However, the knowledge also constrains the orientation of the car so that it can only turn around the z-axis. Thus, the measured x and y accelerations of the IMU never affect the z-velocity. As a consequence, the accelerometer biases of these axes cannot be observable.

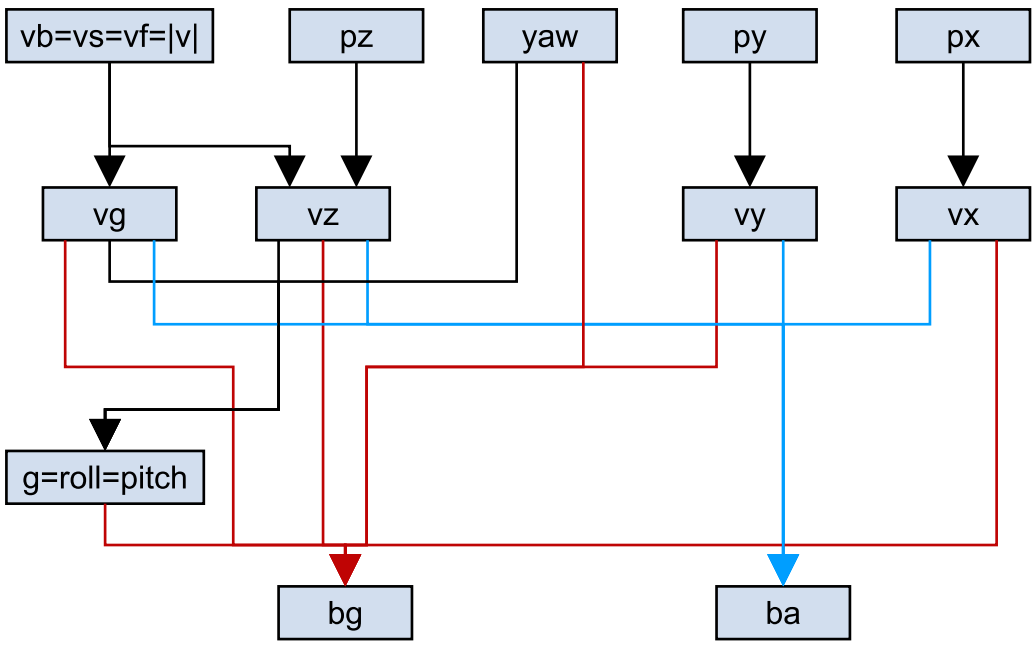

Figure 6: Observability hierarchy for INS. An arrow from state a to b shows that b can get observable if a is known. An equality sign (=) means that the states can yield observability in both directions. Symbols: Ground velocity vg, Gravity direction g, Body velocity vb, Sideway velocity (vehicle constraint) vs, Forward velocity vf, Accelerometer bias ba, Gyrometer bias bg.

The biases are at the lowest level of the hierarchy and can only yield themselves observable. The gyrometer bias can get observable from any orientation or velocity dimension, while the accelerometer bias requires knowledge about a velocity dimension. Interestingly, all three bias dimensions can be observable by one superior state dimension.

The gravity direction can get observable from the ground velocity ($||v_x + v_y||$) or the z-velocity. Knowing the direction of gravity also gives observability of the roll and pitch since this is the inclination. Astonishingly, measuring either the yaw, roll or pitch can also yield the inclination observable.

The world velocity dimensions do not yield observability of each other. The x- and y-velocity only have the corresponding position dimension as ancestors. In consensus with the litera-

ture [95, 96, 99], the ground and z-velocity can get observable from the body, forward, sideways, or norm velocity. The existence of gravity allows distinguishing between velocity along the gravity axis and perpendicular to it. Furthermore, they can yield observability of each other.

The yaw and the position dimensions are at the top of the hierarchy. For INSs, the position can only be observable if it is in the measurement equation since it has no antiderivative state. In contrast, the yaw occurs in the derivatives of the world velocity to rotate the IMU measurements. It does not have a parent in this hierarchy since I only considered a single equation at a time.

I repeated the observability tests with multiple equations at once to test whether there are any synergy effects where multiple equations yield observability of a state that is not observable from a subset of the equations. Interestingly, no synergy effects occur for more than 2 equations. A complete list of the hierarchy can be found in Appendix 11.2.

Most of the synergy effects relate to direct computation rules. Any combination of the ground velocity with either the yaw, the x- or the y-velocity yield the other two. The combination of x- and y-velocity yields the ground velocity and the yaw. Despite these direct relations, the yaw can be observable from knowing the gravity direction and either the x- or y-velocity.

The shown hierarchy emphasizes why map constraints are relevant for INSs. Since they are functions of the position, they may yield observability of the pose of the system. In contrast, knowledge about the velocity can yield observability of the orientation at best.

4 The Human Gait as Prior Distribution

The regular pattern of the human gait is used in the literature as prior knowledge. The stance phase is detected from the IMU data and either a step counting approach or the ZUPT is applied to estimate the velocity [6]. In this chapter, I want to show that the gait can be modeled as a multi-modal prior distribution instead. To achieve this, I adapt the IMM to manifolds so that it can estimate the orientation of the INS. I further develop a manifold EKS and IMMS to improve the results of the estimation. Then, I show a proof of concept that the IMMS can estimate the gait phase and the pose simultaneously by using a narrow Gaussian for the stance and a wide Gaussian for the swing phase. Overall, this chapter shows that conditional DOF knowledge can be modeled as a prior distribution.

4.1 Boxplus Interacting Multiple Model Smoother [IV, V]

The IMM originates from radar tracking of aircraft [88, 106]. Motion models are used to match consecutive radar measurements of the same aircraft, and this allows to track the aircraft with higher accuracy. However, a single motion model cannot represent all possible maneuvers of an aircraft. Thus, different models for straight flight, accelerated flight and turning are deployed.

The IMM can detect which motion mode is most likely. It runs a bank of filters for each possible motion mode and compares their predictions with the measurements. The motion modes are assigned a probability depending on their measurement prediction quality.

Usually, this task yields a sequence of motion modes. The motion mode can change at any time, wherefore new possible sequences emerge at each time step. This is troublesome since the estimator would have to track all possible sequences to find the most likely one. Hence, it would have to manage an ever-growing number of sequences and estimate the state for each of those [43]. Instead, the IMM only tracks the combined probability to be in a mode. This reduces the number of estimated states to a constant. To do this, it mixes the estimates of all filters at every time step.

The IMM is designed for vector states. It mixes the different filter estimates in a weighted sum of Gaussians, using standard vector addition. Unfortunately, the vector addition destroys manifold properties like the unit norm of rotation quaternions. Thus, manifolds cannot be used in the IMM. A possible solution is to normalize the quaternions afterwards [107], but this can negatively impact the estimation of mean and covariance.

To adequately use manifolds in the IMM, we combine it with the $\boxplus$-method (pronounced boxplus). This method has been successfully used to adapt EKF [108], UKF [46] and least-squares estimation [II] to manifold states. It enables the algorithms to handle manifold and vector compound states generically. I review the concept of the method in the next section, while the interested reader can find the mathematical properties in [46] and [V].

4.1.1 Boxplus Manifolds

Manifolds are a special case of equality-constrained spaces, similar to DOF knowledge. For example, rotation quaternions are four real numbers with the additional constraint that their norm is one. Hence, only three numbers would be required since the fourth can be calculated with the constraint. This so-called overparametrization has to be considered in state estimators since any change to the manifold has to satisfy the equality constraint [46].

It is possible to use only as many parameters as the manifold has DOF (three in the case of quaternions). However, these representations have so-called singularities - points where the value on the manifold changes only slightly while the representation jumps. A rotation by $180°$ or $-180°$ results in the same orientation, but the difference in numbers is $360°$. These jumps negatively impact state estimators.

The concept behind the $\boxplus$-method is to represent the manifold with its overparametrization but to express changes with fewer parameters [46]. To avoid the singularity, the changes are expressed relative to the manifold in the so-called tangent space. It can be visualized on a circle manifold (see Figure 7). In the presented case, the tangent space is a line tangential to the circle at a reference r. Infinitesimally close to the reference, the tangent space and the manifold coincide. For higher distances δ, one can find the resulting manifold after a change by projection. This projection is encapsulated in the $\boxplus$-operator. The inverse $\boxminus$-operator (pronounced boxminus) computes the difference between two manifold instances in the tangent space of a reference. The result is the shortest path between them on the manifold, also called the geodesic.

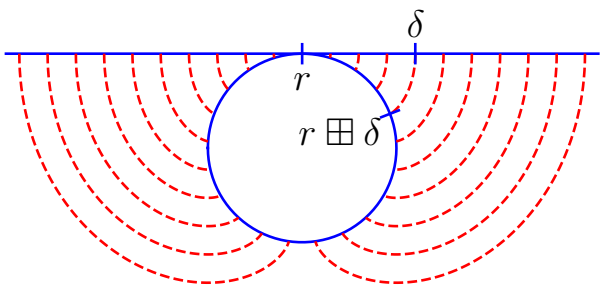

Figure 7: Circular manifold with tangent space (blue line) and a possible $\boxplus$-projection (red lines). Every δ in the tangent space can be projected to a position on the circle.

Knowing the overparametrization, the tangent space and the $\boxplus$- and $\boxminus$-operator is sufficient to adapt Gaussian state estimation algorithms to manifolds [46]. In principle, all operations are performed in the tangent space of the manifold. By using the mean value of the Gaussians as a reference, the singularities are avoided.

4.1.2 Manifold Reference Transform

In the IMM, a filter for each mode of the system is used. Thus, using the $\boxplus$-method would result in multiple different references. That is a challenge because a $\boxplus$-IMM has to combine

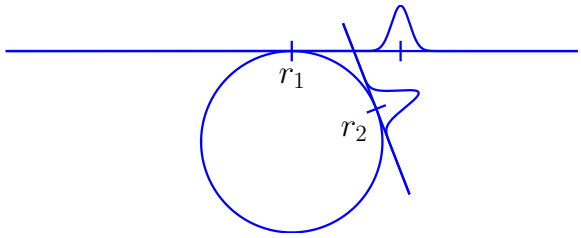

Figure 8: The same Gaussian expressed in two different tangent spaces r_1 and r_2.

Gaussians expressed in different spaces (see Figure 8). A possible solution is to transform all Gaussians to the same reference.

The same Gaussian distribution can have a different covariance if it is expressed with regard to another reference. The reason is that the projection of the $\boxplus$-operator is nonlinear and can shrink distances[3]. In our work [V], we developed a linear approximation to this reference transform.

4.1.3 Boxplus-IMM-Smoothing

With the reference transform, the IMM can be adapted to a $\boxplus$-IMM. All Gaussians are transformed to the same reference and in this tangent space, they can be mixed since it is a vector space. We use the manifold average of the Gaussian means as the reference since it is a linear approximation of the true mean of the combined distribution [IV].

The $\boxplus$-mixing based on reference transforms outperforms the naive approach based on normalization. It has a lower error on the mean and covariance calculation of the mixed Gaussian (see Figure 9). If the Gaussian means are close to each other, the error of both methods is low.

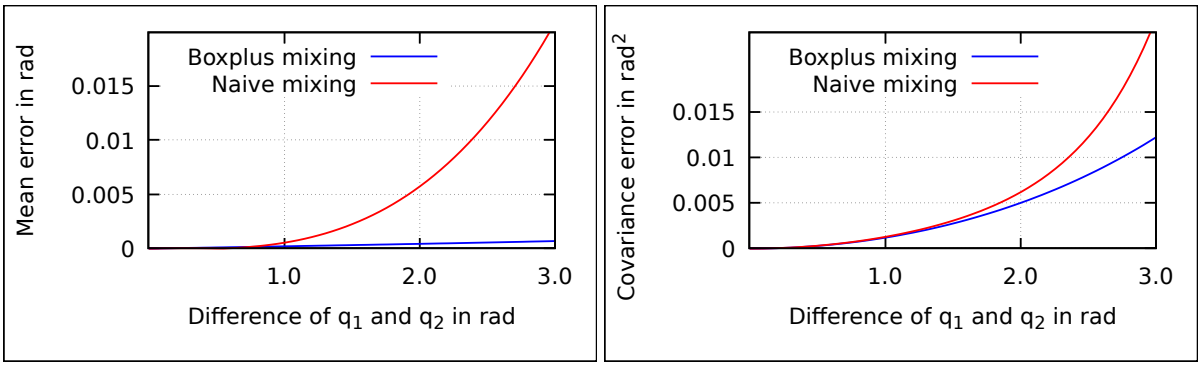

(a) Mean error ($\boxminus$-norm) (b) Covariance error (Schur norm)

Figure 9: Mean and covariance error of boxplus and naive mixing compared to optimal mixing over the angular differences of q_1 and q_2. Reprinted with permission from ref. [IV], Copyright 2020 IEEE.

Based on the reference transforms, a Rauch-Tung-Striebel (RTS)-smoother can also be de-

[3]Precisely, a Gaussian expressed in another reference is not Gaussian anymore due to the nonlinear transform. However, we assume Gaussianity such as in every nonlinear estimator.

rived. Ultimately, the smoothing on ⊞-manifolds only requires performing any computation that requires two different Gaussians in the same tangent space. This results in the ⊞-EKS. The complete derivation can be found in [V]. We combined our manifold smoother with the IMM smoothing of [109] to create the first IMMS on manifolds: The ⊞-IMMS [V].

4.1.4 Evaluation and Discussion

We analyze the performance of the ⊞-EKS, the ⊞-IMM and the ⊞-IMMS on a simulated dataset of an aircraft with an onboard camera. The aircraft performs constant-velocity and constant-turn motion [110], and is localized via known landmarks.

To analyze the performance gain of the reference transforms, we compare to algorithms that differ only in specific details. We use the ⊞-EKF, which is based on the constant-turn model as a baseline estimator for all algorithms. The ⊞-EKS is compared to the Multiplicative Extended Kalman Smoother (MEKS), which is a smoother specifically for quaternions. It only differs from the ⊞-EKS in the covariance smoothing, where it omits the covariance transforms. The ⊞-IMM is compared to a naive IMM (N-IMM), which handles the quaternions like vectors and normalizes after every change [107]. The ⊞-IMMS (⊞-RTSIMMS) is compared to an IMMS that combines both reference algorithms (NM-RTSIMMS).

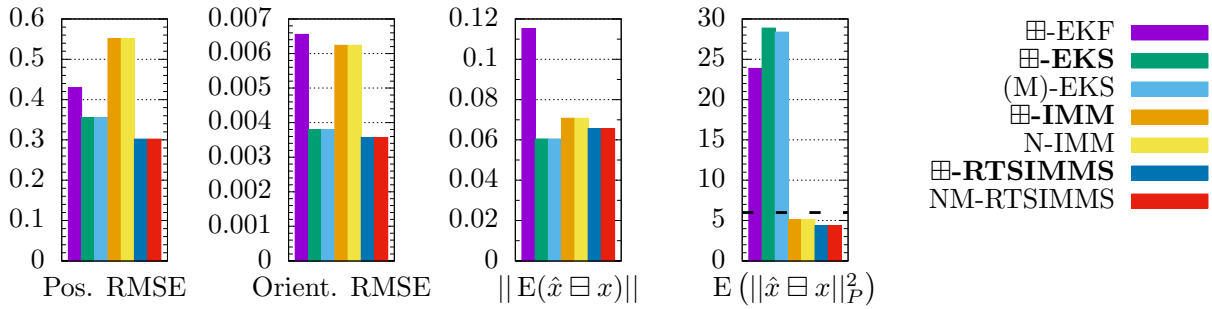

Figure 10: Comparison of ⊞-algorithms and their reference algorithms. The algorithms peform better if the metrics are lower. As an exception, the target value of the consistency measure $\mathrm{E}(||\hat{x} \boxminus x||_P^2)$ is 6 (dashed line). Reprinted from [V] (CC BY 4.0).

The comparison shows that none of the algorithms performs better than the reference (see Figure 10). That is unfortunate since we expect at least an improved covariance estimation through the considered reference transforms. The estimators lack improvement since the different mode estimates are all close to each other in the IMM. Thus, the difference between the linear approximation and the normalization approach has no measurable effect. The reference transform is almost an identity function, at least for the used rotation quaternions.

Nevertheless, the ⊞-algorithms have an advantage over the reference solutions. They are fully generic towards the state and do not need any normalization procedure. Therefore, we combine the ⊞-algorithms with an automatic differentiation framework [111] based on *ceres* [112] to create algorithms that are easy to use and generic[4].

[4]The implementation is available at `https://github.com/TomLKoller/Boxplus-IMM`.

4.2 Prior Modeling of the Gait

The human gait can be modeled as two distinct Gaussian distributions (see Figure 2 in the Introduction). One Gaussian represents the stance phase during the gait. Its mean is zero and it has a low covariance. In principle, this Gaussian models the soft ZUPT.

The second Gaussian represents the swing phase. During the swing, higher velocities occur. Thus, the Gaussian has a high covariance. The covariance of the IMU measurement is much lower, wherefore this Gaussian allows to follow the movement measured by the IMU. The zero mean reduces high-velocity estimates slowly so that the estimate does not raise unrealistically.

The ⊞-IMM is used with an unusual approach. Usually, the dynamic models are different in the IMM, while the measurement is the same for each mode. In this case, I use the standard INS dynamic model without biases[5] for both modes and apply the Gaussians as separate pseudo measurements on the mode filters. This approach allows using the prior distribution in the IMM.

The model has multiple parameters that can be adapted to optimize the estimation. The covariances of the Gaussians and the transition probabilities between the modes can be adapted. In principle, these parameters could be optimized for the gait of each user. The optimal parameters are found by a grid search on real world data based on the position error of the IMM.

4.3 Evaluation and Discussion

The IMM approach is evaluated on the pyShoe dataset [113]. This dataset contains walking trials with continuous ground truth in a room and sparse ground truth in a hallway. In [113], multiple state of the art detectors are implemented, which are used for comparison. I use two different sets of parameters. The first set is optimized on the room dataset[6] and the second on parts of the hallway dataset[7].

The IMM approach can successfully detect the motion pattern of the human gait on the room dataset. The mode probability oscillates between the stance and the swing phase (see Figure 11a). The detected stances of the best detector, according to [113], fall into the stance phase of the IMM. The IMM expects longer stance phases since it does not detect the time point of exactly zero velocity. Instead, it detects low velocity phases in the data.

The IMM detects when the estimated velocity agrees with the prior distribution. Thus, it fails to detect the stance phase if the estimated velocity is inconsistently high for any reason. The IMM cannot detect any further steps, as seen in Figure 11b). That is a major drawback of the approach since it cannot recover from such a state.

If the mode detection of the IMM fails, the position estimate is also impacted. The estimate does not resemble the real trajectory. If the phase detection is successful, the position estimate does look like the true path (see Figure 12a). The position estimate appears to be too short,

[5] Although the biases are theoretically observable from the ZUPT, their estimation is disturbed by the remaining velocity error [26].

[6] Room parameters: Stance Cov.: 0.1, Swing Cov.: 2.0, Transition prob.: 0.271

[7] Hallway parameters: Stance Cov.: 0.1, Swing Cov.: 3.78, stance to swing prob.: 0.5, swing to stance prob.: 0.4

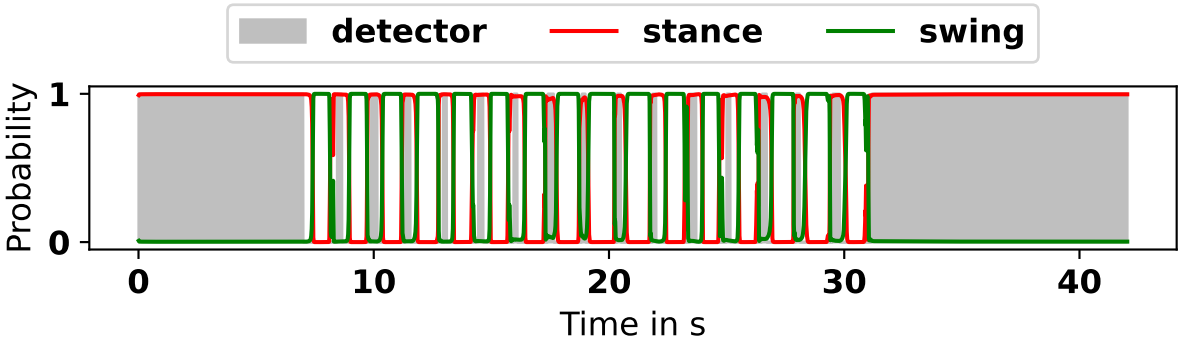

(a) Successful detection of the gait phase

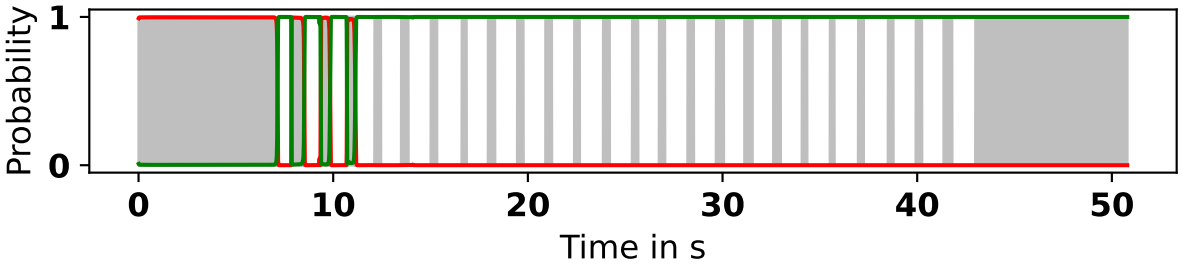

(b) Failure state of the gait phase detection

Figure 11: The mode probability of the IMM approach compared with the best detector according to [113]. The gray background displays when the best detector detects the stance phase. The trials were selected from the room dataset.

i.e., the estimated step length is too small. This results in a slow drift of the position estimate. A possible reason is that the room dataset covers only small walking distances while the hallway dataset contains large distances. With the parameters of the hallway dataset, the step length estimate is corrected almost completely (see Figure 12b).

In Table 2, the IMM and IMMS approach are compared against the LSTM classifier of [114]. The IMM's Averaged RMSE (ARMSE) is higher by at least a factor of two and the IMMS improves the results only slightly. The failure state occurs in trial 2, where the LSTM approach has a high error as well. The IMM approach cannot compete with the state of the art on its current level. However, it is remarkable that the simple prior distribution model achieves results that close to the state of the art. The approach has a high potential for improvement, e.g., by using time-dependent transition probabilities (sojourn time) [73], more accurate phase models or four-phase models of the human gait [80].

Overall, the IMM is an entirely new approach for conditional prior knowledge. The knowledge is modeled as a multi-modal prior distribution and applied as a pseudo measurement instead of an explicit detector. Parameters of the prior distribution model can be retrieved from suitable real-world data. The major drawback of the approach is that it can enter an unrecoverable state where it cannot detect any further steps. The advantage is that the mode detection and state estimation are integrated into one algorithm. This allows to probabilistically handle the

detection so that false detections can be corrected. Although the approach is outperformed by state of the art detector-based approaches, the evaluation shows the potential of the concept to model prior knowledge as prior distribution.

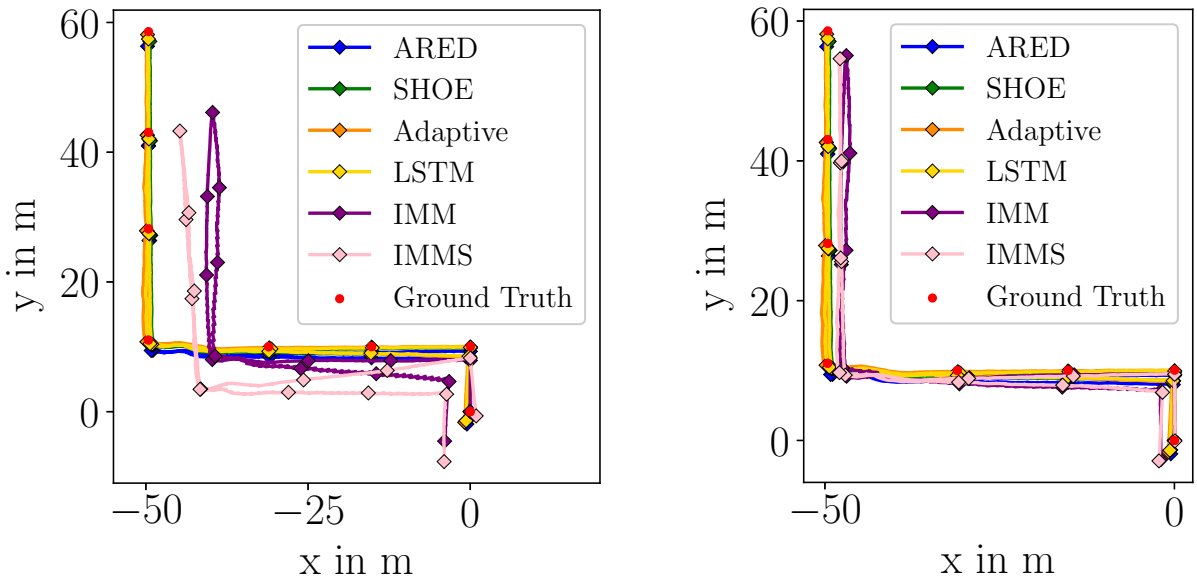

(a) Estimation with room dataset parameters

(b) Estimation with hallway dataset parameters

Figure 12: The position estimate of the IMM approach compared against detector-based approaches for a single trial of the hallway dataset. The pedestrians return to the start.

Table 2: Comparison of the IMM and IMMS approach against the LSTM classifier [114].

Trial #	IMM ARMSE	IMMS ARMSE	LSTM ARMSE
1	1.533	1.495	0.456
2	21.000	17.858	1.746
3	1.228	1.218	0.609
4	1.416	1.360	0.677

5 Terrain Maps as Prior Distribution [I–III]

Terrain maps are a complex constraint on the position. They can also contain information about the heading. Hence, they are a rich source of information for pose estimation. These maps can be used to model streets or vehicle tracks. In the literature, they are used in conjunction with a barometer [22, 23] or transformed into an inclination map [1, 31]. I show that terrain maps can be modeled directly as a prior distribution and used as a pseudo measurement, using track cycling as an example for an indoor application.

5.1 Track Cycling

Track Cycling is an umbrella term for various bicycle races on an indoor track [115]. The athletes compete to be the fastest in sprints or long races. IMU and pose data could be used to rate the athletes' performance for training purposes. A proof of concept study [116] already showed experimentally that the available knowledge in track cycling corrects the position drift.

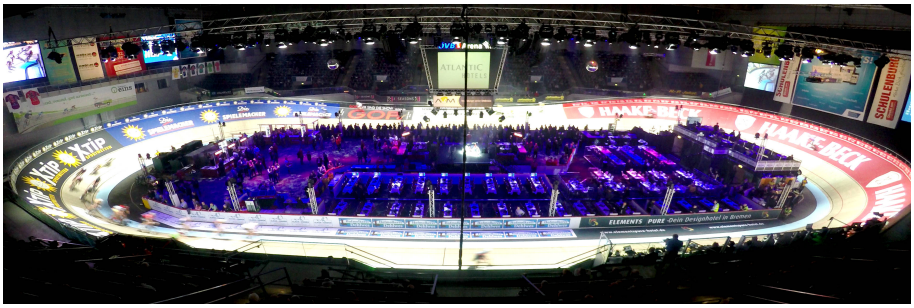

Figure 13: The track of the Sixdays Bremen. Reprinted with permission from [II]. Copyright 2019 IEEE.

Two kinds of knowledge are available about track cycling: The athletes drive on a bike and the bike stays on the track (see Figure 13). Bikes have the wheeled vehicle property that they drive only in their heading direction. Thus, the vehicle constraint can be applied [8]. This can be modeled as unconditional DOF knowledge:

$$v_b = \begin{pmatrix} * \\ 0 \\ 0 \end{pmatrix} + \varepsilon_v, \tag{10}$$

which means that the body velocity v_b is 0 except for the forward direction. Due to slip and drift of the wheels ε_v, the constraint does not hold exactly wherefore it is a soft constraint.

The racing track can be modeled as a terrain map which is again unconditional DOF knowledge. The prior distribution of the state can be modeled as a pseudo measurement. The current height z of the bike has to coincide with the height of the track h at the x, y position:

$$h(x(t), y(t)) - z(t) + \varepsilon_h = 0, \tag{11}$$

where t is the current time. This pseudo measurement models that the bike has zero distance to the track's surface. It has several advantages over the methods in the literature. First, a barometer, as in [22, 23], is not required since the pseudo measurement acts on the state only. Still, it could be fused with a barometer indirectly as it improves the z estimate. Second, the model does not simplify the track to only a portion of its information value. An inclination map, as in [1, 31], would ignore parts of the information gained from the combination of the map and the acceleration measurement of the IMU.

The track consists of two straight parts, which are tilted planes connected by two $180°$ curves (see Figure 13). These curves are shaped cone-like. They are cones except that their inclination depends on the angle [III].

5.2 Observability Analysis

We only use DOF knowledge in the modeling of track cycling. Thus, it is possible to test the observability with standard tests. The observability properties of the non-holonomic vehicle constraint have been analyzed already by [96]. IMU biases, inclination and the velocity magnitude are observable if the vehicle drives a curve. Due to the track's shape, it is given that the bike drives curves. However, the athlete can drive straight on the straight parts. This should cause the estimates of the inclination and velocity to diverge on the straight parts and to be corrected in the curves. The IMU biases evolve slowly, wherefore they should not be affected.

We conduct the observability analysis under the assumption that the IMU biases, inclination and velocity magnitude are observable at all times. As stated, this is wrong in the mathematical sense. However, the information from the curves can be backpropagated to the straight parts, wherefore the error on the states is still low and bounded.

The already known results greatly simplify the observability analysis. Since observability means that a function exists that retrieves the states from the measurements, the states can be assumed to be known for the remaining analysis [III]. Thus, it is only required to prove that using the terrain map yields the position and the heading observable.

We use the test from [38], which requires that the Jacobian of the measurement equations is invertible. It requires as many measurement equations as unobservable states, in this case, four. The first measurement equation is the pseudo measurement (11) and the other three are retrieved by derivation.

The observability has to be analyzed separately for the straight and curved parts. On the straight parts, the heading is observable as long as the bike drives a curve or does not face outward of the track. The intuitive reason for the observability is that the inclination on a tilted plane directly corresponds to the heading. Since the inclination is known the heading can be retrieved.

Due to the complexity of the Jacobian in the curves, we conducted a numerical analysis. The analysis shows that the position and heading are observable in the curves if the biker drives at a constant distance to the curve's center. Since this is a common way to drive, we conclude that the state is observable.

Assuming that the heading is observable, it can be shown analytically that the position is observable in the curves. The assumption is reasonable because the heading is observable on the straight parts and only small heading errors occur due to the gyrometer error. With the known heading, only the three position axes remain unobserved, whereas the measurement derivatives only contain information about the x and y axes. Each row of the Jacobian is the gradient of the pseudo measurement or its derivative with respect to the x and y axes. The state is unobservable if the Jacobian is not invertible, i.e., these gradients must be linearly dependent. Consequently, the gradients of the derivatives are linearly dependent throughout the whole motion, wherefore the whole trajectory can be translated orthogonal to the gradient direction without violating the terrain map knowledge [III]. Ultimately, this means that the state can only be unobservable if the terrain map locally resembles an extrusion of the position trajectory, which is not possible for a trajectory that drives through a complete curve.

Overall, the analysis shows that the pose is reasonably observable with the given knowledge. The mathematical proof shows that the system is not observable on the straight parts. Thus, we expect the error to increase on the straight parts and to reduce in the curves.

5.3 Least-Squares Solution

The knowledge in track cycling is DOF knowledge, wherefore any state estimation that can handle measurements can be applied. The gold standard for this task is the least-squares optimizer since it optimizes the whole trial at once and backpropagates information from later time steps. Backpropagation is important in this application since the position is unobservable on the straight parts.

We model the application as a series of states x_k (4) connected by the INS's dynamic model (5) without using the magnetometer and compute the most likely state sequence with a least-squares estimator based on ceres [112]. The vehicle constraint (10) and the terrain map constraint (11) are applied every step. With this kind of solution, two challenges arise: The positioning of the sensor on the bike and the correct initialisation of the algorithm.

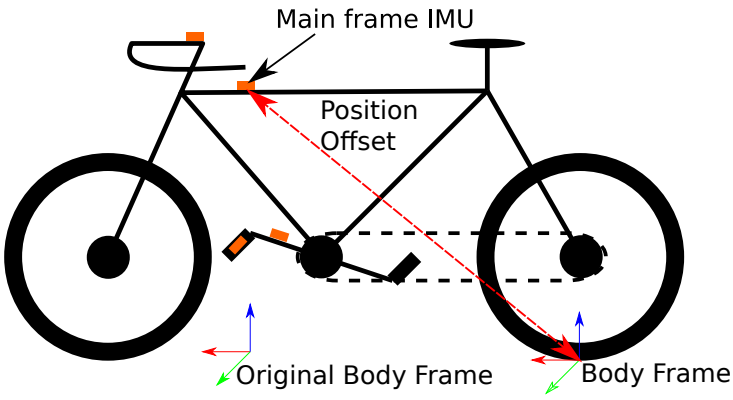

Figure 14: Placements of the IMU on the bike. The measurements of the main frame IMU are transformed to the contact point with the track. Adapted from [III] (CC BY 4.0).

The prior knowledge is only valid for the contact point of the wheels with the track. Other

positions have nonzero distance to the track and can have velocities to the sides due to the tilting of the bike. Unfortunately, the IMU cannot be placed at the contact point. Instead, we place the IMU at the main frame and transform its measurements to the contact point of the back wheel (the body frame, see Figure 14). This is straightforward for the angular rate because it is only a rotation. In contrast, the acceleration is disturbed by the centrifugal and Euler accelerations [117]. These accelerations are induced by the rotational motion and the lever arm between the IMU and the body frame. To correct them, we add the acceleration, angular rate and angular acceleration to the state description. We apply the IMU measurements to these states instead of using them directly in the dynamic model. The centrifugal and Euler accelerations are incorporated into the measurement model. This has the advantage that the undisturbed acceleration at the contact point is estimated.

While least-squares solvers are the gold standard to achieve the best estimate, they suffer from bad initialization states. The reason is that they use gradient descent techniques to find the optimum, which cannot correct the case, where the initial guess skips half a round or more. Thus, a proper initial guess that at least estimates the position down to half-round level is required.

The initial guess can be attained by using a simplified system model. The traveled distance along the track is required as the initial guess. That would place the initial states close enough to the true states to use the gradient descent. Thus, we model the track as a single line, i.e., with zero track width. The line is like a rollercoaster or train rail which defines a relation between the position and the curvature. It can yield observability of the traveled distance [I]. The only condition is that the curvature axis changes, which is true for the track's curves.

To compute the initial guess, we use a line motion model in an UKF smoother and applied the angular rate as a measurement of the current curvature. The simplified system requires huge dynamic noise. The noise effectively models the lateral position error. While this elegantly utilizes the observability of the simplified system, other techniques to compute the initial guess like the moving horizon approach [118] could be applied with less restrictions on the terrain map.

5.4 Dataset and Results

We evaluate the least-squares estimator on a real-world dataset. The dataset contains IMU data of three trials at the Sixdays Bremen track [115]. Each trial is at least 60 rounds ($10\,km$) long. As ground truth, six self-made laser optical barriers measure when the bike passes specific positions. We compare the measured passing time with the computed time based on the pose estimates.

To grasp the meaning of a timing error in position terms, we multiply the time error with the top speed of around $12\,m/s$. The average RMSE is $1.08\,m$ which shows the capability of the method. The error does not increase over time which shows that the terrain map corrects the drift. A video with the projected estimate[8] shows qualitatively that the error increases on the

[8] The video can be found at `http://www.informatik.uni-bremen.de/agebv/zavi`.

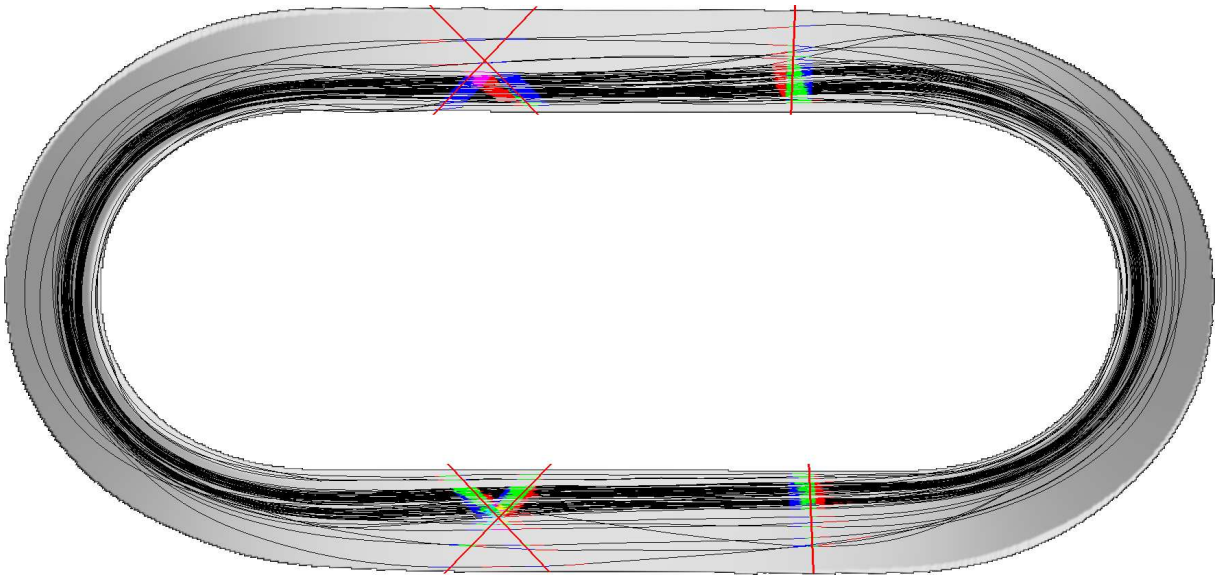

Figure 15: Trajectory of a biker in the first trial after 100 iterations of the optimizer. The optical barriers are shown as red lines. The red color indicates that the bike actually passes a barrier (measurement), whereas blue indicates that the estimator predicts that the bike passes a barrier. The green color shows where prediction and measurement agree. Reprinted from [III] (CC BY 4.0).

straights and decreases on the curves, as expected from the observability analysis.

Initially, we transformed the IMU measurements to the position on the track beneath the IMU instead of the contact point of the back wheel [II] (see Figure 14). This violates the vehicle constraint as it does not hold for that position during turns [119]. As a consequence, the RMSE increases to $1.15\,m$.

5.5 Discussion

With track cycling, we showed experimentally and mathematically that the position can get fully observable from a terrain map without additional sensors. Interestingly, the pose observability is conditional, while the knowledge of the terrain map and the vehicle constraint is not. The straight parts yield information about the heading, which is a main factor in the position drift. In the curves, the INS's drift is corrected. Therefore, it is required to reason about the error on the straight parts. If the athlete drives straight on it, not even the velocity is observable, which could cause a strong drift. The drift is only limited by the information gained from the curved parts. Thus, long and slow drives on the straight part cause high errors. However, these occur rarely during a race.

Conceptually, our approach is similar to the inclination map in [1, 31]. The inclination map seems to be advantageous over a terrain map, since the inclination can be observed from an IMU combined with the vehicle constraint. Our work shows that the estimator can infer the pose from the position prior itself. Thus, terrain maps can be used as the prior distribution of the position directly.

The initial evaluation with the wrong body frame shows that it is essential to model the knowledge accurately. The original body frame violates the vehicle constraint in curves. As a consequence, the pseudo measurement is systematically biased, which increases the error.

Simplifying the track to an 1D route allows computing a suitable initial guess. The lateral position is not relevant for the initial guess, wherefore the simplification is feasible. However, the used strategy only works for terrain maps that can be seen as a route. For open spaces, approaches like the Moving Horizon Estimator (MHE) could be used.

To sum it up, this work has shown that terrain maps can yield full observability of the pose, and thus, correct the position drift using only the accelerometer and gyrometer. The approach to model the maps as a prior distribution and to use this as a pseudo measurement is shown to be effective. It allows using standard state estimators and standard observability tests. Thus, any advancement of these methods can be applied to terrain maps.

6 Event-Domain Maps as Prior Distribution [VI]

Like terrain maps, event-domain maps contain information about the position and the heading. However, they cannot be modeled as Gaussian pseudo measurements since they are multi-modal. The same event may correspond to multiple locations in the world. In the literature, this is handled with HMMs [25]. The movement between two detected events is estimated from the IMU measurements. It is used to compute how likely the system moves from one landmark to another based on the moved distance. In principle, the Viterbi algorithm [120] matches the movements to the event-domain map and extracts the most likely sequence of landmarks. Instead, I model the event-domain map as a multi-modal prior distribution on the position and fuse it with the measured movements of the IMU. I evaluate the methodology on bouldering as an application example because the movements are limited to a small area which is easy to track with ground truth sensors.

6.1 Bouldering

Bouldering is a climbing sport without downfall protection other than gym mats. It has received scientific interest in the last decade. The sport has been enhanced by augmented reality projected on the wall [121] and a camera that tracks movements. This enables climbers to project self-designed routes or the shadow of more experienced climbers in order to learn from them [121], or to dodge virtual chainsaws in gamification approaches [122]. Performance parameters can be accessed through wearables at the wrists [123]. They also allow detecting the climbed route, which is interesting for the administration of the boulder gym [124]. The data can be used to decide which routes are replaced or restructured.

Furthermore, bouldering is an exciting example of event-domain maps. The climbers need to grip at holds or wall features to climb up (see Figure 16). Thus, their hands do not only stop movement, but they are also restricted to a subset of the whole state space. In contrast to the event landmarks in PAC, the bouldering holds are close to each other, which should enable precise tracking of the position.

Bouldering presents an additional challenge since the event of gripping at a hold may not be distinguishable from other events. Climbers can support themselves by placing their hands against the wall. Furthermore, the topology of holds does allow gripping at different positions and orientations at the same hold. Thus, a point landmark is insufficient to model every possible hold.

6.2 Observability Analysis

Since the hands stop when the climber grips a hold, a ZUPT can be used. Thus, the biases of the IMU, the magnitude of the velocity and the inclination are observable [99]. The position and heading remain unobserved.

Unfortunately, the domain knowledge cannot be analyzed with the classical observability tests. In theory, a position measurement yields observability of the position and heading. How-

Figure 16: Bouldering with inertial sensors at the hands, feet and hip. The sensors are tracked with infrared motion capture markers that provide ground truth position. Only the hand sensors are used in the current study. Extracted from the dataset of [VI] (CC BY-NC 4.0).

ever, it cannot be detected unambiguously at which hold the hand is or whether it is at a hold at all. Thus, the system can only be observable if the correct sequence of grips can be extracted.

6.3 Divided-Estimation Solution

Event-domain maps are challenging prior knowledge. They are multi-modal and non-Gaussian. Thus, Kalman filter based algorithms or least-squares can hardly be used to estimate the position. A Particle Filter (PF) is the usual approach to solve this kind of constraint. Since the PF represents the estimate with a large number of particles, it can handle almost any kind of information. The problem is that the INS has a relatively large state dimension of 18, wherefore a PF would need an immense amount of particles to represent it accurately.

This problem is solved in both PDR and PAC by dividing the state estimation. As a first step, the IMU data is used together with the gait knowledge to estimate single steps and their heading. These are further combined to transitions between event landmarks for PAC. The retrieved transitions are fused with the map or landmark information in a second stage estimator. PDR uses PFs to handle the binary nature of the building maps [7]. In PAC, it is common to use HMMs, where the transitions are used to calculate the hidden state transition probabilities [25].

We generalized the concept of dividing the estimation to apply it to conditional domain knowledge. The dividing itself has the drawback that information from the domain knowledge does not improve the estimates of states in the first estimation. In PAC, this is done artificially by recalculating the step length based on the transition length between event landmarks [25], while it is ignored in PDR. Actually, the information propagation can be dropped if the states are

already estimated well. Our idea is to estimate only the observable states in the first step. If the states are already observable without the domain knowledge, we expect that the estimation has only minor errors that accumulate in the position. In this example, the observable states coincide with the transition states (everything except position and heading). Overall, we use a 3-step methodology:

1. Detector Stage: The relevant events are detected, which results in a detector function $d(k)$ that is 1 when the conditional domain knowledge is applicable and otherwise 0.

2. Transition Estimation: The observable states between two detected events are estimated.

3. Domain Sampling: The unobservable states are sampled and refined by the conditional domain knowledge.

This methodology is a concept to create divided-estimation solutions for conditional domain knowledge applications. It does not dictate which algorithms have to be used. In general, every classifier can be used as the detector. Since the transition estimation is bound to observable unimodal states, the same algorithms as for DOF knowledge can be used. In domain sampling, any sampling approach like the PF or Bayesian Occupancy Grid (BOG) filters can be used as long as they can represent the multi-modal distribution of the knowledge.

For bouldering, we applied a moving window approach that thresholds on the acceleration's standard deviation [125] as the detector. Again, the transition estimator is a least-squares estimator as in the track cycling application. Instead of the vehicle constraint, the ZUPT is used at every time step with a detected grip. Since the heading is not observable from the measurements, we added the magnetometer measurement as a heading reference. The magnetometer is prone to magnetic disturbances, but it corrects the ever-growing drift.

For domain sampling, we use a PF smoother that can backpropagate information. It can localize at which hold a trial started. This is usually ambiguous because most routes have two start handles and it is not regulated which hand starts at which handle.

As stated, the climbers are not limited to gripping at the holds but can grip anywhere on the wall. Thus, there is a small probability that gripping does not occur at a hold. We modeled this as a uniform probability to grip anywhere. Gripping holds themselves is modeled as a ball set around the center since it is unknown how the athletes grip exactly. We smoothed out the sets with Gaussian tails to account for the border's ambiguity.

To combine the probabilities of the different grip positions, we use a maximum logic, i.e., only the highest likelihood is used. This models that the participant can only grip at one position at once. Thus, each particle implicitly represents a whole sequence of grip positions rather than the cumulative probability of being at a position regardless of the sequence. That is similar to the HMM method in PAC, which extracts the most likely sequence of event landmarks via the Viterbi algorithm [25]. To account for the multi-modal distribution, the PF clusters the particles based on the last grip position and outputs the mean of the most likely cluster.

6.4 Dataset and Results

To evaluate the methodology, we collected a dataset with 27 participants who performed over 750 trials. The dataset contains IMU data of the hands, feet and hip. It contains ground truth positions via infrared markers and video data of the trial. The participants gave their written consent to publish their data open access so that this dataset is the first open access dataset for bouldering [9].

Twelve different routes were recorded, including a self-designed route to force dynamic jumps to reach the holds. The PF smoother achieves a median error of $0.132m$ on the dataset (see Table 3). The smoother greatly reduces the error compared to the transition estimation with a median error of $0.266m$. While the median error is promising, there are many trials where the tracking fails, i.e., where the wrong sequence of holds is estimated.

Table 3: Results of the transition estimator, PF and PF smoother. Adapted from [VI].

Algorithm	25% Qtl.	Median	75% Qtl.	RMSE	Max
Transition	0.125	0.266	0.544	0.560	6.135
PF	0.108	0.145	0.320	0.441	4.265
PF smoother	0.101	0.132	0.231	0.413	4.265

The tracking can fail due to different reasons [VI]. While most of these have technical reasons (sensor errors, magnetic disturbances, particle depletion) two issues relate to the observability. Uncompleted trials, i.e., when the participants stop before reaching the top, have much higher errors than completed trials. These trials contain fewer transitions, wherefore the start handle often stays ambiguous.

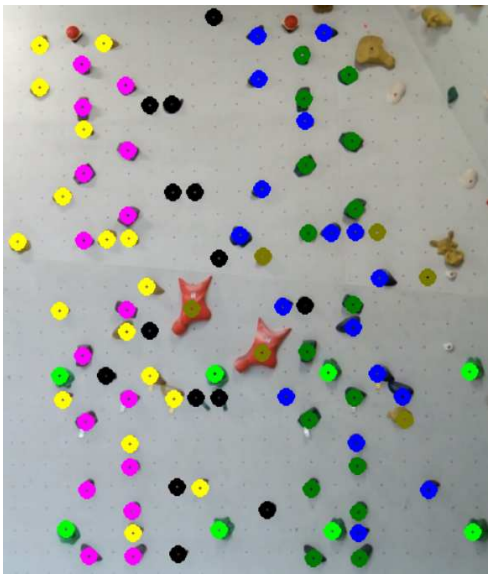

Figure 17: Routes of the first climb wall in the study. The ground truth map of the routes is projected onto the holds.

[9] Download at `http://www.informatik.uni-bremen.de/zavi-datasets/info.html`.

The second issue appears on the dark green route (see Figure 17). The route is built of two vertical lines of holds. The starting handle is often estimated wrongly, even in completed trials. A possible reason is that the athletes only climb vertically with their hands so that both routes have a reasonable probability. However, the issue does not appear on the purple route which is almost identical.

6.5 Discussion

The value of the conditional domain knowledge lies in the transitions between the domains. As seen in the experiments, trials with only a few transitions contain insufficient information to determine the true position. The reason is that other paths with the same transitions are possible. This finding directly relates to a possible concept of observability: A sequence of landmark positions is only observable if there is no other path with similar transitions. While this seems simple, the similarity between paths is dependent on the noise of the transition estimation.

Our divided approach sets a new focus on the observability of the states. Observable states are estimated in the transition estimation. Although we call it the transition estimation, not all transition states are observable. For example, the heading error introduced by magnetic disturbances is unobservable. Unobservable states are sampled in the PF. This allows using the full transition rather than the traveled distance only and to refine the unobservable transition states probabilistically. SHS could also benefit from this divided approach. While the step count is measured, the heading and the step length could be sampled in the PF.

Modeling the event-domain map as a multi-modal prior distribution has led to a PF-based solution. Compared to the HMM approach [25], it has the advantage that arbitrary prior distributions are usable. Thus, event locations can be modeled with more detail than a point location. Bouldering would be challenging to solve with HMMs since the possibility to grip at other places than the known landmarks exists. In the PF, this can be modeled straightforwardly with the prior distribution. Overall, our approach allows for more general event-domain maps while it preserves the maximum likelihood logic of the HMM approach. Unfortunately, particle depletion can occur. The PF may fail to estimate the true position sequence due to this algorithmic failure rather than insufficient information.

The PF approach is advantageous in applications with additional information. For example, in PDR not only the event-domain map constrains the position. The building map also constrains the position between landmarks. While HMMs cannot apply building maps, it is straightforward in the PF. Thus, conditional and unconditional domain knowledge can be fused to improve the estimation in future work.

In essence, our approach enables using event-domain maps probabilistically with the well-studied PF. Arbitrary distributions are applicable without increasing the algorithmic complexity. If the grip sequence is extracted correctly, the position drift can be reduced. Yet again, modeling the knowledge as a prior distribution leads to an effective pose estimator based on standard methods.

7 Conclusion

In this thesis, I studied the usage of prior knowledge with IMUs. This topic is studied extensively in the literature with various types of knowledge and applications. Often, the prior knowledge is modeled as a prior probability distribution. I followed this concept and applied it to three types of knowledge where it has not been applied entirely: The human gait, terrain maps and event-domain maps. As a result, the contribution of this work is twofold: New applications solely based on inertial sensors and prior knowledge are presented and the algorithmic integration of the prior knowledge is generalized.

Up to now, the knowledge about the human gait has been used in detector-based approaches [6]. This work presents a new approach to model the gait as a multi-modal prior distribution. Based on this model, the gait phase and the pose are estimated simultaneously in a manifold IMM. The necessary IMM and its smoother have been developed and tested on a real-world dataset. The result is a new class of state estimators for conditional DOF knowledge.

Two sports — track cycling and bouldering — were investigated in this thesis. Datasets were collected and published open-access to evaluate the estimators in challenging real world scenarios. In both applications, the INS's drift is corrected by a map and knowledge about the velocity. Thus, the IMU is the only required sensor. The knowledge is applied using suitable standard state estimators, namely a least-squares estimator and the PF. The estimated pose and velocity are valuable to access the performance of the athletes automatically or by a coach.

For track cycling, the terrain map has been generalized to a pseudo measurement on the position. This generalization could be used with any terrain map without transforming to an inclination map as in [1, 31]. This work presents the first formal proof of observability for terrain maps with INS. Thus, it proves that terrain maps can yield observability of the pose. Extrusion shapes are an exception since they contain ambiguities that render the pose unobservable, wherefore additional sensors would be required. However, further measurements can be fused with the knowledge straightforwardly since a standard state estimator is used.

For bouldering, the grip positions were modeled as an event-domain map. This map type is a generalization of the landmark maps in PAC [25, 74], which are used to match detected events to landmarks. In this work, a divided-estimator solution based on least-squares estimation and the PF has been developed to handle arbitrary distributions of the event-domain. Thus, the approach is usable for all kinds of event-domain maps of any application. Furthermore, the methodology enables fusing the maps with all kinds of measurements and knowledge; either in the transition estimation or the domain sampling.

Overall, I successfully applied the concept of prior knowledge as prior probability distributions on different types of knowledge. In each case, the knowledge is fused with the IMU measurements by generic state estimation algorithms and each example application was solved adequately. This showcases the capability of the concept to aid INS with prior knowledge. Even complex map knowledge is applicable with standard state estimators so that the position drift is corrected. Therefore, this work has shown that modeling prior knowledge as prior distribution is a standardized approach to integrating knowledge in sensor fusion.

8 Future Work

Although all implementations were tested on real-world data, this thesis aimed to showcase general concepts rather than solving specific applications. Thus, the shown solutions have the potential for improvements.

The failure state of the IMM approach for human gait estimation is currently non-recoverable. It is possible that the current modeling of the gait is overly simplified. That could cause the failure state since the estimator cannot cover the real world motions. The modeling could be improved with other pseudo measurement models, e.g., a model with positive velocity norm, or by adding more models for other gait patterns like running. Detailed models have a high value in this approach since they may improve not only the state estimate but also the phase estimate. Furthermore, non-Gaussian models could be used by adapting the current $\boxplus$-IMM to use a PF for each mode. However, it might be necessary to resort to a specialized routine to recover from the failure state.

Beside the human gait, the IMM approach could be used for stationary modes in general [60, 84, 85]. It is also thinkable to apply it to inline skating, where the stance phase follows the vehicle model rather than a ZUPT.

In the track cycling study, we already showed that a lever arm between the surface and the IMU position can be compensated. In particular, this is necessary for vehicles since the IMU can hardly be positioned at the surface contact. One could investigate whether it is possible to compensate for more advanced lever arms. For example, in [93], an IMU is placed in the pedal and used to estimate the velocity based on the cadence. It is effectively an odometer that does not rely on curved motion. The better observability of the velocity on the straight parts could improve the position estimate if this changing lever arm can be compensated.

As already stated, the MHE may be used to compute the initial guess in track cycling instead of the ad-hoc initial guess via the line model. The MHE could be used instead of the least-squares optimizer to enable online estimation. A real-time capable system could be used for cars during GNSS [1, 31] outages or in track cycling itself to access the state of the race automatically.

The event-domain map in bouldering has improved the tracking of the hands in the dataset. Unfortunately, it is currently impossible to analyze the observability of domain knowledge theoretically. Possibly, an observability criterion based on set theory [126, 127] can be used in the future to identify challenging room configurations.

With the presented methodology, event-domain maps, as in PAC, could be combined with building maps. That could improve the tracking accuracy since the transitions between landmarks would be constrained further.

Conditional domain knowledge like event-domain maps is underrepresented in the literature compared to the other classes. It has a high potential for new state estimation schemes. It may be used to detect on which floor an elevator is exited, or to track climbing stairs. Since arbitrary prior distributions can be used, whole rooms could be used as landmarks if they have

any detectable features. For example, the floor type identification of [90] could be used for this purpose. Furthermore, additional sensors could be used if the event or the distinctive property cannot be detected in the IMU data. The arbitrary distributions also allow using statistical user behavior which is influenced by the environment. For example, pedestrians may slow down at bottlenecks in a building [128].

All things considered, this thesis contributes general approaches to use prior knowledge. Hereafter, they should be deployed in new applications based on inertial sensors.

9 My Publications

[I] T. L. Koller, T. Laue, and U. Frese. “State Observability through Prior Knowledge: A Conceptional Paradigm in Inertial Sensing.” In: *Proceedings of the 16th International Conference on Informatics in Control, Automation and Robotics (ICINCO)*. 2019.
My Contribution: 85%
I performed the observability proof for rollercoasters and discussed several aspects of prior knowledge.

[II] T. L. Koller and U. Frese. “State Observability through Prior Knowledge: Tracking Track Cyclers with Inertial Sensors.” In: *2019 International Conference on Indoor Positioning and Indoor Navigation (IPIN)*. 2019 International Conference on Indoor Positioning and Indoor Navigation (IPIN). 2019.
My Contribution: 90%
I prepared the ground truth sensors and recorded the dataset with the help of my student Lukas Post. I modeled the knowledge, implemented the least squares optimizer and evaluated the results.

[III] T. L. Koller and U. Frese. “State Observability through Prior Knowledge: Analysis of the Height Map Prior for Track Cycling.” In: *Sensors* 20.9 (9 2020), p. 2438.
My Contribution: 90%
I implemented an improvement of the prior publication and performed the full observability proof.

[IV] T. L. Koller and U. Frese. “The Interacting Multiple Model Filter on Boxplus-Manifolds.” In: *2020 IEEE International Conference on Multisensor Fusion and Integration for Intelligent Systems (MFI)*. 2020 IEEE International Conference on Multisensor Fusion and Integration for Intelligent Systems (MFI). 2020, pp. 88–93.
My Contribution: 90%
I derived the IMM on manifolds, implemented it and evaluated it in a self-written simulation. I analyzed the lack of improvement against the naive normalization approach.

[V] T. L. Koller and U. Frese. “The Interacting Multiple Model Filter and Smoother on Boxplus-Manifolds.” In: *Sensors* 21.12 (12 2021), p. 4164.
My Contribution: 90%
I performed the derivation of the manifold smoother, implemented it and evaluated the results. I analyzed the lack of improvement compared to other approaches.

[VI] T. L. Koller, T. Laue, and U. Frese. “Event-Domain Knowledge in Inertial Sensor Based State Estimation of Human Motion.” In: *Proceedings of the 25th International Conference on Information Fusion. FUSION 2022.* in press.
My Contribution: 85%
I prepared the ground truth sensors with my students Lukas Post, Timo Wörner and Andreas Baude. I planned, advertised and performed the experiments with the partici-

pants. I devised and implemented the splitted estimator solution and evaluated it on the dataset.

[VII] J. Clemens, C. Wellhausen, T. L. Koller, U. Frese, and K. Schill. “Kalman Filter with Moving Reference for Jump-Free, Multi-Sensor Odometry with Application in Autonomous Driving.” In: *2020 IEEE 23rd International Conference on Information Fusion (FUSION)*. 2020 IEEE 23rd International Conference on Information Fusion (FUSION). 2020, pp. 1–9.
My Contribution: 5%
I was asked for advise and contributed small portions to the written paper.

10 Literature

[1] A. Dean, R. Martini, and S. Brennan. “Terrain-Based Road Vehicle Localisation Using Particle Filters.” In: *Vehicle System Dynamics* 49.8 (8 2011), pp. 1209–1223.

[2] A. Basiri, E. S. Lohan, T. Moore, A. Winstanley, P. Peltola, C. Hill, P. Amirian, and P. Figueiredo e Silva. “Indoor Location Based Services Challenges, Requirements and Usability of Current Solutions.” In: *Computer Science Review* 24 (2017), pp. 1–12.

[3] P. Davidson and R. Piché. “A Survey of Selected Indoor Positioning Methods for Smartphones.” In: 19.2 (2 2017), p. 24.

[4] D. Vecchia, P. Corbalán, T. Istomin, and G. P. Picco. “TALLA: Large-scale TDoA Localization with Ultra-wideband Radios.” In: *2019 International Conference on Indoor Positioning and Indoor Navigation (IPIN)*. 2019 International Conference on Indoor Positioning and Indoor Navigation (IPIN). 2019, pp. 1–8.

[5] R. Amsters, D. Holm, J. Joly, E. Demeester, N. Stevens, and P. Slaets. “Visible Light Positioning Using Bayesian Filters.” In: *Journal of Lightwave Technology* 38.21 (2020), pp. 5925–5936.

[6] R. Harle. “A Survey of Indoor Inertial Positioning Systems for Pedestrians.” In: *IEEE Communications Surveys Tutorials* 15.3 (3 2013), pp. 1281–1293.

[7] O. Woodman and R. Harle. “Pedestrian Localisation for Indoor Environments.” In: *Proceedings of the 10th International Conference on Ubiquitous Computing* (Seoul, Korea). UbiComp ’08. New York, NY, USA: ACM, 2008, pp. 114–123.

[8] G. Dissanayake, S. Sukkarieh, E. Nebot, and H. Durrant-Whyte. “The Aiding of a Low-Cost Strapdown Inertial Measurement Unit Using Vehicle Model Constraints for Land Vehicle Applications.” In: *IEEE Transactions on Robotics and Automation* 17.5 (5 2001), pp. 731–747.

[9] B. Pannetier, K. Benameur, V. Nimier, and M. Rombaut. “VS-IMM Using Road Map Information for a Ground Target Tracking.” In: *2005 7th International Conference on Information Fusion*. 2005 7th International Conference on Information Fusion. Philadelphia, PA, USA: IEEE, 2005, 8 pp.

[10] G. Battistello, M. Ulmke, F. Papi, M. Podt, and Y. Boers. “Assessment of Vessel Route Information Use in Bayesian Non-Linear Filtering.” In: *2012 15th International Conference on Information Fusion*. 2012, pp. 447–454.

[11] S. Challa and N. Bergman. “Target Tracking Incorporating Flight Envelope Information.” In: *Proceedings of the Third International Conference on Information Fusion*. Proceedings of the Third International Conference on Information Fusion. Paris, France: IEEE, 2000, THC2/22–THC2/27 vol.2.

[12] F. Wenk and U. Frese. “Posture from Motion.” In: *2015 IEEE/RSJ International Conference on Intelligent Robots and Systems (IROS)*. 2015 IEEE/RSJ International Conference on Intelligent Robots and Systems (IROS). 2015, pp. 280–285.

[13] Forssell, Urban, P. Hall, S. Ahlqvist, and F. Gustafsson. “Map-Aided Positioning System.” In: *Citeseer*. Proceedings, International Federation of Automotive Engineering Societies (2002).

[14] S. Beauregard, Widyawan, and M. Klepal. “Indoor PDR Performance Enhancement Using Minimal Map Information and Particle Filters.” In: *2008 IEEE/ION Position, Location and Navigation Symposium*. 2008, pp. 141–147.

[15] M. Podt, M. Bootsveld, Y. Boers, and F. Papi. “Exploiting Imprecise Constraints in Particle Filtering Based Target Tracking.” In: *17th International Conference on Information Fusion (FUSION)*. 2014, pp. 1–8.

[16] J. Racko, P. Brida, A. Perttula, J. Parviainen, and J. Collin. “Pedestrian Dead Reckoning with Particle Filter for Handheld Smartphone.” In: *2016 International Conference on Indoor Positioning and Indoor Navigation (IPIN)*. 2016 International Conference on Indoor Positioning and Indoor Navigation (IPIN). 2016, pp. 1–7.

[17] R. Toledo-Moreo, M. A. Zamora-Izquierdo, and A. F. Gomez-Skarmeta. “Multiple Model Based Lane Change Prediction for Road Vehicles with Low Cost GPS/IMU.” In: *2007 IEEE Intelligent Transportation Systems Conference*. 2007 IEEE Intelligent Transportation Systems Conference. 2007, pp. 473–478.

[18] D. Streller. “Road Map Assisted Ground Target Tracking.” In: *2008 11th International Conference on Information Fusion*. 2008 11th International Conference on Information Fusion. 2008, pp. 1–7.

[19] H. Sadruddin and M. M. Atia. “Fusion of Digital Road Maps with Inertial Sensors and Satellite Navigation Systems Using Kalman Filter and Hidden Markov Models.” In: *Sensors & Transducers* 237.9 (9 2019), pp. 129–136.

[20] J. Liu, B. Cai, J. Wang, and W. Shangguan. “GNSS/INS-based Vehicle Lane-Change Estimation Using IMM and Lane-Level Road Map.” In: *16th International IEEE Conference on Intelligent Transportation Systems (ITSC 2013)*. 16th International IEEE Conference on Intelligent Transportation Systems (ITSC 2013). 2013, pp. 148–153.

[21] J. López-Araquistain, Á. J. Jarama, J. A. Besada, G. de Miguel, and J. R. Casar. “A New Approach to Map-Assisted Bayesian Tracking Filtering.” In: *Information Fusion* 45 (2019), pp. 79–95.

[22] T. Sonmez and H. E. Bingol. “Modeling and Simulation of a Terrain Aided Inertial Navigation Algorithm for Land Vehicles.” In: *2008 IEEE/ION Position, Location and Navigation Symposium*. 2008 IEEE/ION Position, Location and Navigation Symposium. 2008, pp. 1046–1052.

[23] C. Mandel and T. Laue. “Particle Filter-based Position Estimation in Road Networks Using Digital Elevation Models.” In: *2010 IEEE/RSJ International Conference on Intelligent Robots and Systems*. 2010 IEEE/RSJ International Conference on Intelligent Robots and Systems (IROS 2010). Taipei: IEEE, 2010, pp. 5744–5749.

[24] L. A. H. Horita, A. Przewodowski, T. C. dos Santos, and F. S. Osorio. “Altitude Offset Constraint for Mobile Robots’ Localization.” In: *2020 IEEE 23rd International Conference on Intelligent Transportation Systems (ITSC)*. 2020 IEEE 23rd International Conference on Intelligent Transportation Systems (ITSC). Rhodes, Greece: IEEE, 2020, pp. 1–6.

[25] B. Zhou, Q. Li, Q. Mao, W. Tu, and X. Zhang. “Activity Sequence-Based Indoor Pedestrian Localization Using Smartphones.” In: *IEEE Transactions on Human-Machine Systems* 45.5 (5 2015), pp. 562–574.

[26] J.-O. Nilsson, I. Skog, and P. Handel. “A Note on the Limitations of ZUPTs and the Implications on Sensor Error Modeling.” In: *International Conference on Indoor Positioning and Indoor Navigation* (2012).

[27] S. J. Julier and J. J. LaViola. “On Kalman Filtering With Nonlinear Equality Constraints.” In: *IEEE Transactions on Signal Processing* 55.6 (6 2007), pp. 2774–2784.

[28] D. Simon. “Kalman Filtering with State Constraints: A Survey of Linear and Nonlinear Algorithms.” In: *IET Control Theory & Applications* 4.8 (8 2010), pp. 1303–1318.

[29] F. Papi, M. Podt, Y. Boers, G. Battistello, and M. Ulmke. “On Constraints Exploitation for Particle Filtering Based Target Tracking.” In: *2012 15th International Conference on Information Fusion*. 2012 15th International Conference on Information Fusion. 2012, pp. 455–462.

[30] N. Amor, G. Rasool, and N. C. Bouaynaya. *Constrained State Estimation - A Review*. 2018. URL: http://arxiv.org/abs/1807.03463 (visited on 02/16/2022).

[31] X. Zhu, C. Qiu, and M. A. Minor. “Terrain-inclination-based Three-dimensional Localization for Mobile Robots in Outdoor Environments.” In: *Journal of Field Robotics* 31.3 (2014), pp. 477–492.

[32] A. Doucet and A. M. Johansen. “A Tutorial on Particle Filtering and Smoothing: Fifteen Years Later.” In: *Handbook of nonlinear filtering* 12 (2009), pp. 656–704.

[33] T. Kirubarajan, Y. Bar-Shalom, K. Pattipati, I. Kadar, B. Abrams, and E. Eadan. “Tracking Ground Targets with Road Constraints Using an IMM Estimator.” In: *1998 IEEE Aerospace Conference Proceedings (Cat. No.98TH8339)*. 1998 IEEE Aerospace Conference. Proceedings. Vol. 5. Snowmass at Aspen, CO, USA: IEEE, 1998, pp. 5–12.

[34] M. Tahk and J. Speyer. “Target Tracking Problems Subject to Kinematic Constraints.” In: *IEEE Transactions on Automatic Control* 35.3 (1990), pp. 324–326.

[35] A. Benavoli, L. Chisci, A. Farina, S. Immediata, and L. Timmoneri. “Knowledge-Based Radar Tracking.” In: *Knowledge-Based Radar Detection, Tracking, and Classification*. Ed. by F. Gini and M. Rangaswamy. Hoboken, NJ, USA: John Wiley & Sons, Inc., 2007, pp. 167–196.

[36] J. Taylor. “The Cramér-Rao Estimation Error Lower Bound Computation for Deterministic Nonlinear Systems.” In: *IEEE Transactions on Automatic Control* 24.2 (1979), pp. 343–344.

[37] A. Martinelli. *Observability: A New Theory Based on the Group of Invariance*. SIAM, 2020. 277 pp.

[38] J. Adamy. *Nichtlineare Systeme Und Regelungen*. Springer, 2018.

[39] A. Martinelli. *Rank Conditions for Observability and Controllability for Time-varying Nonlinear Systems*. 2020. URL: http://arxiv.org/abs/2003.09721 (visited on 07/24/2020).

[40] J. E. Pascoe. "The Inverse Function Theorem and the Jacobian Conjecture for Free Analysis." In: *Mathematische Zeitschrift* 278.3-4 (3-4 2014), pp. 987–994.

[41] J. Breßler, P. Reisdorf, M. Obst, and G. Wanielik. "GNSS Positioning in Non-Line-of-Sight Context—A Survey." In: *2016 IEEE 19th International Conference on Intelligent Transportation Systems (ITSC)*. 2016 IEEE 19th International Conference on Intelligent Transportation Systems (ITSC). 2016, pp. 1147–1154.

[42] J. A. Hesch, D. G. Kottas, S. L. Bowman, and S. I. Roumeliotis. "Camera-IMU-based Localization: Observability Analysis and Consistency Improvement." In: *The International Journal of Robotics Research* 33.1 (1 2014), pp. 182–201.

[43] M. Hofbaur and B. Williams. "Hybrid Estimation of Complex Systems." In: *IEEE Transactions on Systems, Man, and Cybernetics, Part B (Cybernetics)* 34.5 (5 2004), pp. 2178–2191.

[44] N. Lovren and J. Pieper. "A Strapdown Inertial Navigation System for the Flat-Earth Model." In: *IEEE Transactions on Aerospace and Electronic Systems* 33.1 (1997), pp. 214–224.

[45] U. Qureshi and F. Golnaraghi. "An Algorithm for the In-Field Calibration of a MEMS IMU." In: *IEEE Sensors Journal* 17.22 (2017), pp. 7479–7486.

[46] C. Hertzberg, R. Wagner, U. Frese, and L. Schröder. "Integrating Generic Sensor Fusion Algorithms with Sound State Representations through Encapsulation of Manifolds." In: *Information Fusion* 14.1 (1 2013), pp. 57–77.

[47] Y. Bar-Shalom, X. R. Li, and T. Kirubarajan. *Estimation with Applications to Tracking and Navigation: Theory Algorithms and Software*. John Wiley & Sons, 2004. 584 pp.

[48] J. Diebel. "Representing Attitude: Euler Angles, Unit Quaternions, and Rotation Vectors." In: *Matrix* 58 (2006), pp. 1–35.

[49] O.-O. Christidi-Loumpasefski, K. Nanos, and E. Papadopoulos. "On Parameter Estimation of Space Manipulator Systems Using the Angular Momentum Conservation." In: *2017 IEEE International Conference on Robotics and Automation (ICRA)*. 2017 IEEE International Conference on Robotics and Automation (ICRA). 2017, pp. 5453–5458.

[50] J. Li, G. Taylor, and D. B. Kidner. "Accuracy and Reliability of Map-matched GPS Coordinates: The Dependence on Terrain Model Resolution and Interpolation Algorithm." In: *Computers & Geosciences* 31.2 (2005), pp. 241–251.

[51] M. Koivisto, H. Nurminen, S. Ali-Loytty, and R. Piche. “Graph-Based Map Matching for Indoor Positioning.” In: *2015 10th International Conference on Information, Communications and Signal Processing (ICICS)*. 2015 10th International Conference on Information, Communications and Signal Processing (ICICS). Singapore: IEEE, 2015, pp. 1–5.

[52] D. Veillard, F. Mailly, and P. Fraisse. “EKF-based State Estimation for Train Localization.” In: *2016 IEEE SENSORS*. 2016 IEEE SENSORS. 2016, pp. 1–3.

[53] L. Xu, Y. Liang, Q. Pan, Z. Duan, and G. Zhou. “A Kinematic Model of Route-Based Target Tracking: Direct Discrete-Time Form.” In: *2016 19th International Conference on Information Fusion (FUSION)*. 2016, pp. 225–231.

[54] C. Mandel and O. Birbach. “Localization in Urban Environments by Matching Sensor Data to Map Information.” In: *2013 European Conference on Mobile Robots*. 2013 European Conference on Mobile Robots (ECMR). Barcelona, Catalonia, Spain: IEEE, 2013, pp. 50–55.

[55] D. A. Castanon, B. C. Levy, and A. S. Willsky. “Algorithms for the Incorporation of Predictive Information in Surveillance Theory.” In: *International Journal of Systems Science* 16.3 (1985), pp. 367–382.

[56] K. Li, C. Zhou, and G. Zhou. “State Estimation Using a Destination Constraint with Uncertainty.” In: *2018 IEEE Radar Conference (RadarConf18)*. 2018 IEEE Radar Conference (RadarConf18). Oklahoma City, OK: IEEE, 2018, pp. 333–338.

[57] M. Angermann and P. Robertson. “FootSLAM: Pedestrian Simultaneous Localization and Mapping Without Exteroceptive Sensors—Hitchhiking on Human Perception and Cognition.” In: *Proceedings of the IEEE* 100.Special Centennial Issue (Special Centennial Issue 2012), pp. 1840–1848.

[58] T. Seel, J. Raisch, and T. Schauer. “IMU-Based Joint Angle Measurement for Gait Analysis.” In: *Sensors* 14.4 (4 2014), pp. 6891–6909.

[59] F. Wenk. “Inertial Motion Capturing Rigid Body Pose and Posture Estimation with Inertial Sensors.” PhD thesis. University of Bremen, 2017.

[60] M. Miezal, B. Taetz, and G. Bleser. “Real-Time Inertial Lower Body Kinematics and Ground Contact Estimation at Anatomical Foot Points for Agile Human Locomotion.” In: *2017 IEEE International Conference on Robotics and Automation (ICRA)*. 2017 IEEE International Conference on Robotics and Automation (ICRA). Singapore, Singapore: IEEE, 2017, pp. 3256–3263.

[61] T. von Marcard, B. Rosenhahn, M. J. Black, and G. Pons-Moll. “Sparse Inertial Poser: Automatic 3D Human Pose Estimation from Sparse IMUs.” In: *Computer Graphics Forum* 36.2 (2 2017), pp. 349–360.

[62] V. Helma and M. Goubej. “Active Anti-Sway Crane Control Using Partial State Feedback from Inertial Sensor.” In: *2021 23rd International Conference on Process Control (PC)*. 2021 23rd International Conference on Process Control (PC). Strbske Pleso, Slovakia: IEEE, 2021, pp. 137–142.

[63] X. Xu, Y. Sun, X. Tian, L. Zhou, and Y. Li. “An Encoder-Free Joint Velocity Estimation Method for Serial Manipulators Using Inertial Sensors.” In: *2021 IEEE International Conference on Robotics and Automation (ICRA)*. 2021 IEEE International Conference on Robotics and Automation (ICRA). 2021, pp. 1566–1571.

[64] B. Paden, M. Čáp, S. Z. Yong, D. Yershov, and E. Frazzoli. “A Survey of Motion Planning and Control Techniques for Self-Driving Urban Vehicles.” In: *IEEE Transactions on Intelligent Vehicles* 1.1 (1 2016), pp. 33–55.

[65] I. Klein, S. Filin, and T. Toledo. “Pseudo-Measurements as Aiding to INS during GPS Outages.” In: *Navigation* 57.1 (1 2010), pp. 25–34.

[66] F. Papi, M. Bocquel, M. Podt, and Y. Boers. “Fixed-Lag Smoothing for Bayes Optimal Exploitation of External Knowledge.” In: *2012 15th International Conference on Information Fusion*. 2012 15th International Conference on Information Fusion. 2012, pp. 463–470.

[67] M. Morgado, P. Oliveira, C. Silvestre, and J. F. Vasconcelos. “Embedded Vehicle Dynamics Aiding for USBL/INS Underwater Navigation System.” In: *IEEE Transactions on Control Systems Technology* 22.1 (2014), pp. 322–330.

[68] J. Pinchin, C. Hide, and T. Moore. “A Particle Filter Approach to Indoor Navigation Using a Foot Mounted Inertial Navigation System and Heuristic Heading Information.” In: *2012 International Conference on Indoor Positioning and Indoor Navigation (IPIN)*. 2012 International Conference on Indoor Positioning and Indoor Navigation (IPIN). Sydney, Australia: IEEE, 2012, pp. 1–10.

[69] D. Zachariah, I. Skog, M. Jansson, and P. Handel. “Bayesian Estimation With Distance Bounds.” In: *IEEE Signal Processing Letters* 19.12 (2012), pp. 880–883.

[70] I. Skog, J.-O. Nilsson, D. Zachariah, and P. Handel. “Fusing the Information from Two Navigation Systems Using an Upper Bound on Their Maximum Spatial Separation.” In: *2012 International Conference on Indoor Positioning and Indoor Navigation (IPIN)*. 2012 International Conference on Indoor Positioning and Indoor Navigation (IPIN). Sydney, Australia: IEEE, 2012, pp. 1–5.

[71] S. O. H. Madgwick, A. J. L. Harrison, and R. Vaidyanathan. “Estimation of IMU and MARG Orientation Using a Gradient Descent Algorithm.” In: *2011 IEEE International Conference on Rehabilitation Robotics*. 2011 IEEE International Conference on Rehabilitation Robotics. 2011, pp. 1–7.

[72] E. Sviestins and V. Pirard. “Constraint Aware Dynamics in Target Tracking.” In: *Proceedings of the 16th International Conference on Information Fusion*. Proceedings of the 16th International Conference on Information Fusion. 2013, pp. 572–579.

[73] Z. Tian, M. Cen, Y. Li, and H. Zhu. “Ground Vehicle Tracking Using Context-Based Sojourn Time Dependent Markov Model and Pseudo-Measurement.” In: *IEEE Access* 8 (2020), pp. 111536–111552.

[74] S. Khalifa, M. Hassan, and A. Seneviratne. “Adaptive Pedestrian Activity Classification for Indoor Dead Reckoning Systems.” In: *International Conference on Indoor Positioning and Indoor Navigation*. International Conference on Indoor Positioning and Indoor Navigation. 2013, pp. 1–7.

[75] S. Khalifa, M. Hassan, and A. Seneviratne. “Feature Selection for Floor-Changing Activity Recognition in Multi-Floor Pedestrian Navigation.” In: *2014 Seventh International Conference on Mobile Computing and Ubiquitous Networking (ICMU)*. 2014 Seventh International Conference on Mobile Computing and Ubiquitous Networking (ICMU). 2014, pp. 1–6.

[76] S. Jingjing, R. Mingrong, W. Pu, and M. Juan. “Indoor Pedestrian Positioning Algorithm with Feature Point Detection and Virtual Path Matching.” In: *2017 Chinese Automation Congress (CAC)*. 2017 Chinese Automation Congress (CAC). 2017, pp. 6567–6571.

[77] R. Jackermeier and B. Ludwig. “Smartphone-Based Activity Recognition in a Pedestrian Navigation Context.” In: *Sensors* 21 (2021), p. 3243.

[78] J. W. Kim, H. J. Jang, D.-H. Hwang, and C. Park. “A Step, Stride and Heading Determination for the Pedestrian Navigation System.” In: *Journal of Global Positioning Systems* (2004), p. 7.

[79] F. Cavallo, A. Sabatini, and V. Genovese. “A Step toward GPS/INS Personal Navigation Systems: Real-Time Assessment of Gait by Foot Inertial Sensing.” In: *2005 IEEE/RSJ International Conference on Intelligent Robots and Systems*. 2005 IEEE/RSJ International Conference on Intelligent Robots and Systems. Edmonton, Alta., Canada: IEEE, 2005, pp. 1187–1191.

[80] J.-S. Wang, C.-W. Lin, Y.-T. C. Yang, and Y.-J. Ho. “Walking Pattern Classification and Walking Distance Estimation Algorithms Using Gait Phase Information.” In: *IEEE Transactions on Biomedical Engineering* 59.10 (2012), pp. 2884–2892.

[81] B. Zhou, Q. Li, Q. Mao, W. Tu, X. Zhang, and L. Chen. “ALIMC: Activity Landmark-Based Indoor Mapping via Crowdsourcing.” In: *IEEE Transactions on Intelligent Transportation Systems* 16.5 (2015), pp. 2774–2785.

[82] S. Grzonka, A. Karwath, F. Dijoux, and W. Burgard. “Activity-Based Estimation of Human Trajectories.” In: *IEEE Transactions on Robotics* 28.1 (2012), pp. 234–245.

[83] M. Hardegger, D. Roggen, and G. Tröster. “3D ActionSLAM: Wearable Person Tracking in Multi-Floor Environments.” In: *Personal and Ubiquitous Computing* 19.1 (1 2015), pp. 123–141.

[84] A. Ramanandan, A. Chen, and J. A. Farrell. “Inertial Navigation Aiding by Stationary Updates.” In: *IEEE Transactions on Intelligent Transportation Systems* 13.1 (1 2012), pp. 235–248.

[85] E. Foxlin. “Pedestrian Tracking with Shoe-Mounted Inertial Sensors.” In: *IEEE Computer Graphics and Applications* 25.6 (6 2005), pp. 38–46.

[86] M. Schmidt, E. Meyer, and T. Jaitner. “Quantifying Jump-Specific Loads in Beach Volleyball by an Inertial Measurement Device.” In: *International Journal of Sports Science & Coaching* 16.2 (2021), pp. 391–397.

[87] M. Koifman and I. Bar-Itzhack. “Inertial Navigation System Aided by Aircraft Dynamics.” In: *IEEE Transactions on Control Systems Technology* 7.4 (1999), pp. 487–493.

[88] X. Li and Y. Bar-Shalom. “Design of an Interacting Multiple Model Algorithm for Air Traffic Control Tracking.” In: *IEEE Transactions on Control Systems Technology* 1.3 (3 1993), pp. 186–194.

[89] T. J. Debus, P. E. Dupont, and R. D. Howe. “Contact State Estimation Using Multiple Model Estimation and Hidden Markov Models.” In: *The International Journal of Robotics Research* 23.4-5 (4-5 2004), pp. 399–413.

[90] Y. Wang and A. M. Shkel. “Learning-Based Floor-Type Identification in the ZUPT-Aided Pedestrian Inertial Navigation.” In: *IEEE Sensors Letters* 5.3 (2021), pp. 1–4.

[91] X. Niu, Y. Li, J. Kuang, and P. Zhang. “Data Fusion of Dual Foot-Mounted IMU for Pedestrian Navigation.” In: *IEEE Sensors Journal* 19.12 (12 2019), pp. 4577–4584.

[92] T. Lew, T. Emmei, D. D. Fan, T. Bartlett, A. Santamaria-Navarro, R. Thakker, and A.-a. Agha-mohammadi. *Contact Inertial Odometry: Collisions Are Your Friends*. 2019. URL: `http://arxiv.org/abs/1909.00079` (visited on 03/15/2022).

[93] J. Cockcroft, J. H. Muller, and C. Scheffer. “A Complementary Filter for Tracking Bicycle Crank Angles Using Inertial Sensors, Kinematic Constraints, and Vertical Acceleration Updates.” In: *IEEE Sensors Journal* 15.8 (2015), pp. 4218–4225.

[94] K. Abdulrahim, C. Hide, T. Moore, and C. Hill. “Aiding Low Cost Inertial Navigation with Building Heading for Pedestrian Navigation.” In: *Journal of Navigation* 64.2 (2011), pp. 219–233.

[95] X. Niu, Y. Li, Q. Zhang, Y. Cheng, and C. Shi. “Observability Analysis of Non-Holonomic Constraints for Land-Vehicle Navigation Systems.” In: *Journal of Global Positioning Systems* 11.1 (2012), pp. 80–88.

[96] Y. Rothman, I. Klein, and S. Filin. “Analytical Observability Analysis of INS with Vehicle Constraints.” In: *Navigation: Journal of The Institute of Navigation* 61.3 (3 2014), pp. 227–236.

[97] D. Roetenberg, H. Luinge, and P. Slycke. “Xsens MVN: Full 6DOF Human Motion Tracking Using Miniature Inertial Sensors.” In: *Xsens Motion Technol. BV Tech. Rep.* 3 (2009).

[98] K. Eckhoff, M. Kok, S. Lucia, and T. Seel. “Sparse Magnetometer-free Inertial Motion Tracking – A Condition for Observability in Double Hinge Joint Systems.” In: *IFAC-PapersOnLine* 53 (2020), pp. 16023–16030.

[99] A. Ramanandan, A. Chen, and J. A. Farrell. “Inertial Navigation Aiding by Stationary Updates.” In: *IEEE Transactions on Intelligent Transportation Systems* 13.1 (2012), pp. 235–248.

[100] D. Tedaldi, A. Pretto, and E. Menegatti. “A Robust and Easy to Implement Method for IMU Calibration without External Equipments.” In: *2014 IEEE International Conference on Robotics and Automation (ICRA)*. 2014 IEEE International Conference on Robotics and Automation (ICRA). 2014, pp. 3042–3049.

[101] W. Ali, Y. Li, M. A. Z. Raja, and N. Ahmed. “Generalized Pseudo Bayesian Algorithms for Tracking of Multiple Model Underwater Maneuvering Target.” In: *Applied Acoustics* 166 (2020), p. 107345.

[102] H. A. P. Blom. “An Efficient Filter for Abruptly Changing Systems.” In: *The 23rd IEEE Conference on Decision and Control*. The 23rd IEEE Conference on Decision and Control. Las Vegas, Nevada, USA, USA, 1984, pp. 656–658.

[103] J. D. Glass, W. D. Blair, and Y. Bar-Shalom. “IMM Estimators with Unbiased Mixing for Tracking Targets Performing Coordinated Turns.” In: *2013 IEEE Aerospace Conference*. 2013 IEEE Aerospace Conference. 2013, pp. 1–10.

[104] K. Krishanth, R. Tharmarasa, T. Kirubarajan, P. Valin, and E. Meger. “Prediction and Retrodiction Algorithms for Path-Constrained Targets.” In: *IEEE Transactions on Aerospace and Electronic Systems* 50.4 (2014), pp. 2746–2761.

[105] N. Amor, N. C. Bouaynaya, R. Shterenberg, and S. Chebbi. “On the Convergence of Constrained Particle Filters.” In: *IEEE Signal Processing Letters* 24.6 (2017), pp. 858–862.

[106] H. A. P. Blom. “An Efficient Filter for Abruptly Changing Systems.” In: *The 23rd IEEE Conference on Decision and Control*. The 23rd IEEE Conference on Decision and Control. Las Vegas, Nevada, USA, USA, 1984, pp. 656–658.

[107] C.-D. Wann and J.-H. Gao. “Orientation Estimation for Sensor Motion Tracking Using Interacting Multiple Model Filter.” In: *IEICE TRANSACTIONS on Fundamentals of Electronics, Communications and Computer Sciences* E93-A.8 (8 2010), pp. 1565–1568.

[108] J. Clemens and K. Schill. “Extended Kalman Filter with Manifold State Representation for Navigating a Maneuverable Melting Probe.” In: *2016 19th International Conference on Information Fusion (FUSION)*. 2016 19th International Conference on Information Fusion (FUSION). 2016, pp. 1789–1796.

[109] N. Nadarajah, R. Tharmarasa, M. McDonald, and T. Kirubarajan. “IMM Forward Filtering and Backward Smoothing for Maneuvering Target Tracking.” In: *IEEE Transactions on Aerospace and Electronic Systems* 48.3 (3 2012), pp. 2673–2678.

[110] Ronghui Zhan and Jianwei Wan. “Passive Maneuvering Target Tracking Using 3D Constant-Turn Model.” In: *2006 IEEE Conference on Radar*. 2006 IEEE Conference on Radar. 2006.

[111] Lukas Post. “Ein Framework zur automatischen Differenzierung von Extended Kalman Filtern auf Mannigfaltigkeiten.” Master thesis. University of Bremen, 2020.

[112] S. Agarwal, K. Mierle, et al. *Ceres Solver*. URL: http://ceres-solver.org.

[113] B. Wagstaff, V. Peretroukhin, and J. Kelly. “Robust Data-Driven Zero-Velocity Detection for Foot-Mounted Inertial Navigation.” In: *IEEE Sensors Journal* 20.2 (2020), pp. 957–967.

[114] B. Wagstaff and J. Kelly. “LSTM-Based Zero-Velocity Detection for Robust Inertial Navigation.” In: *2018 International Conference on Indoor Positioning and Indoor Navigation (IPIN)*. 2018 International Conference on Indoor Positioning and Indoor Navigation (IPIN). 2018, pp. 1–8.

[115] *SIXDAYS BREMEN — Die Einzigartige Verbindung von Sport Und Unterhaltung*. URL: https://sixdays.de/ (visited on 03/29/2022).

[116] T. Laue, U. Frese, and L. Post. “State Estimation Solely based on Inertial Sensing and Prior Knowledge.” In: *Sportinformatik XII – 12. Symposium der dvs-Sektion ”Sportinformatik und Sporttechnologie” vom 5.-7. September 2018 in Garching. Abstracts.* Ed. by D. Link, A. Hermann, M. Lames, and V. Senner. Vol. 274. Schriften der Deutschen Vereinigung für Sportwissenschaft. 2018, pp. 96–97.

[117] H. Carlsson, I. Skog, G. Hendeby, and J. Jaldén. *Inertial Navigation Using an Inertial Sensor Array*. 2022. URL: http://arxiv.org/abs/2201.11983 (visited on 05/17/2022).

[118] T. Polóni, B. Rohal-Ilkiv, and T. Arne Johansen. “Moving Horizon Estimation for Integrated Navigation Filtering.” In: *IFAC-PapersOnLine* 48.23 (23 2015), pp. 519–526.

[119] T. Yeh, H.-T. Lu, and P.-H. Tseng. “Balancing Control of a Self-driving Bicycle.” In: *Proceeding of the 16th International Conference on Informatics in Control, Automation and Robotics (ICINCO 2019(*. ICINCO. Vol. 2. Praha, Czech Republic: SCITEPRESS, 2019, pp. 34–41.

[120] G. Forney. “The Viterbi Algorithm.” In: *Proceedings of the IEEE* 61.3 (1973), pp. 268–278.

[121] F. Kosmalla, F. Daiber, F. Wiehr, and A. Krüger. “ClimbVis: Investigating In-situ Visualizations for Understanding Climbing Movements by Demonstration.” In: *Proceedings of the 2017 ACM International Conference on Interactive Surfaces and Spaces*. ISS ’17. New York, NY, USA: Association for Computing Machinery, 2017, pp. 270–279.

[122] R. Kajastila and P. Hämäläinen. “Augmented Climbing: Interacting with Projected Graphics on a Climbing Wall.” In: *CHI ’14 Extended Abstracts on Human Factors in Computing Systems*. CHI EA ’14. Toronto, Ontario, Canada: Association for Computing Machinery, 2014, pp. 1279–1284.

[123] F. Kosmalla, F. Wiehr, F. Daiber, A. Krüger, and M. Löchtefeld. “ClimbAware: Investigating Perception and Acceptance of Wearables in Rock Climbing.” In: *Proceedings of the 2016 CHI Conference on Human Factors in Computing Systems*. CHI ’16. New York, NY, USA: Association for Computing Machinery, 2016, pp. 1097–1108.

[124] A. Kalyanaraman, J. Ranjan, and K. Whitehouse. “Automatic Rock Climbing Route Inference Using Wearables.” In: *Adjunct Proceedings of the 2015 ACM International Joint Conference on Pervasive and Ubiquitous Computing and Proceedings of the 2015 ACM International Symposium on Wearable Computers*. UbiComp/ISWC’15 Adjunct. Osaka, Japan: Association for Computing Machinery, 2015, pp. 41–44.

[125] C. Ladha, N. Y. Hammerla, P. Olivier, and T. Plötz. “ClimbAX: Skill Assessment for Climbing Enthusiasts.” In: *Proceedings of the 2013 ACM International Joint Conference on Pervasive and Ubiquitous Computing*. UbiComp ’13. New York, NY, USA: Association for Computing Machinery, 2013, pp. 235–244.

[126] E. López, L. M. Gómez, and H. Alvarez. “A Set-Theoretic Approach to Observability and Its Application to Process Control.” In: *Journal of Process Control* 80 (2019), pp. 15–25.

[127] E. López, J. Hahn, L. M. Gómez, and H. Alvarez. “Input Trajectory Design for the Enhancement of State Estimation through a Set-Theoretic Approach to Observability.” In: *Industrial & Engineering Chemistry Research* 59.30 (30 2020), pp. 13631–13641.

[128] A. Seyfried, O. Passon, B. Steffen, M. Boltes, T. Rupprecht, and W. Klingsch. “New Insights into Pedestrian Flow Through Bottlenecks.” In: *Transportation Science* 43.3 (2009), pp. 395–406.

11 Appendix

11.1 Continuous Linear Input Dynamic Model of an INS

$$g(x,\vec{a}_I,\vec{\omega}_I) = f_0(x) + \begin{pmatrix} f_1(x) & f_2(x) & f_3(x) \end{pmatrix} * \vec{a}_I + \begin{pmatrix} f_4(x) & f_5(x) & f_6(x) \end{pmatrix} * \vec{\omega}_I$$

$$f_0 = \begin{pmatrix} 0.5 q_W^I * \begin{pmatrix} 0 \\ -\vec{b}_g \end{pmatrix} \\ \vec{v}_W \\ q_W^I * (-\vec{b}_a) + \vec{g} \\ \vec{0}_{9\times 1} \end{pmatrix}$$

$$f_1(x) = \begin{pmatrix} 0_{7\times 1} \\ q_W^I * \begin{pmatrix} 1 \\ 0 \\ 0 \end{pmatrix} * \overline{q}_W^I \\ 0_{9\times 1} \end{pmatrix}, \quad f_2(x) = \begin{pmatrix} 0_{7\times 1} \\ q_W^I * \begin{pmatrix} 0 \\ 1 \\ 0 \end{pmatrix} * \overline{q}_W^I \\ 0_{9\times 1} \end{pmatrix}, \quad f_3(x) = \begin{pmatrix} 0_{7\times 1} \\ q_W^I * \begin{pmatrix} 0 \\ 0 \\ 1 \end{pmatrix} * \overline{q}_W^I \\ 0_{9\times 1} \end{pmatrix}$$

$$f_4(x) = \begin{pmatrix} 0.5 q_W^I * \begin{pmatrix} 0 \\ 1 \\ 0 \\ 0 \end{pmatrix} \\ 0_{15\times 1} \end{pmatrix}, \quad f_5(x) = \begin{pmatrix} 0.5 q_W^I * \begin{pmatrix} 0 \\ 0 \\ 1 \\ 0 \end{pmatrix} \\ 0_{15\times 1} \end{pmatrix}, \quad f_6(x) = \begin{pmatrix} 0.5 q_W^I * \begin{pmatrix} 0 \\ 0 \\ 0 \\ 1 \end{pmatrix} \\ 0_{15\times 1} \end{pmatrix}$$

11.2 Full Observability Hierarchy for multiple Equations

Notation:
$a > b \mapsto$ a may yield observability of b;
$a = b \mapsto$ a and b may yield observability of each other;
$[a,b] \mapsto$ groups a and b.

[pz,Ground velocity]$>$ [Body velocity,Non-Holonomic,Forward v,$|v|$]
[vz,Ground velocity]$=$ [Body velocity,Non-Holonomic,Forward v,$|v|$]

[vx,Ground velocity]$>$ [vy,Yaw]
[vy,Ground velocity]$>$ [vx,Yaw]

[px,py]$>$ [Ground velocity,Gravity direction,Roll,Pitch,Yaw]
[px,vy]$>$ [Ground velocity,Gravity direction,Roll,Pitch,Yaw]
[py,vx]$>$ [Ground velocity,Gravity direction,Roll,Pitch,Yaw]

[Ground velocity,Yaw]=[vx,vy]
[$|v|$,Yaw]> [vx,vy]
[Body velocity,Yaw]> [vx,vy]
[Forward v,Yaw]> [vx,vy]
[Non-Holonomic,Yaw]> [vx,vy]

[Body velocity,vy]> [vx,Yaw]
[Non-Holonomic,vy]> [vx,Yaw]
[Forward v,vy]> [vx,Yaw]
[$|v|$,vy]> [vx,Yaw]
[Body velocity,vx]> [vy,Yaw]
[Non-Holonomic,vx]> [vy,Yaw]
[Forward v,vx]> [vy,Yaw]
[$|v|$,vx]> [vy,Yaw]

[px,Body velocity]> [vy,Yaw]
[px,Non-Holonomic]> [vy,Yaw]
[px,Forward v]> [vy,Yaw]
[px,$|v|$]> [vy,Yaw]
[px,Ground velocity]> [vy,Yaw]

[py,Ground velocity]> [vx,Yaw]
[py,Body velocity]> [vx,Yaw]
[py,Non-Holonomic]> [vx,Yaw]
[py,Forward v]> [vx,Yaw]
[py,$|v|$]> [vx,Yaw]

[px,Gravity direction]> [Yaw]
[px,Roll]> [Yaw]
[px,Pitch]> [Yaw]
[vx,Gravity direction]> [Yaw]
[vx,Roll]> [Yaw]
[vx,Pitch]> [Yaw]

[py,Gravity direction]> [Yaw]
[py,Roll]> [Yaw]
[py,Pitch]> [Yaw]
[vy,Gravity direction]> [Yaw]
[vy,Roll]> [Yaw]
[vy,Pitch]> [Yaw]
[py,pz]> [Yaw]
[py,vz]> [Yaw]

[vz,vy]> [Yaw]
[pz,vy]> [Yaw]
[pz,vx]> [Yaw]
[vz,vx]> [Yaw]
[px,vz]> [Yaw]
[px,pz]> [Yaw]